Catena 196 (2021) 104865

Contents lists available at ScienceDirect

Catena

journal homepage: www.elsevier.com/locate/catena

Analysing hydrological and sediment transport regime in two Mediterranean intermittent rivers

Josep Fortesa[a,b], Giovanni Francesco Ricci[c,*], Julián García-Comendador[a,b], Francesco Gentile[c], Joan Estrany[a,b], Eric Sauquet[d], Thibault Datry[d], Anna Maria De Girolamo[e]

[a] Mediterranean Ecogeomorphological and Hydrological Connectivity Research Team, Department of Geography, University of the Balearic Islands, Ctra. Valldemossa km 7.5, 07122 Palma, Balearic Islands, Spain
[b] Institute of Agro-Environmental and Water Economy Research—INAGEA, University of the Balearic Islands, Ctra. Valldemossa km 7.5, 07122 Palma, Balearic Islands, Spain
[c] Department of Agricultural and Environmental Sciences, University of Bari Aldo Moro, 70126 Bari, Italy
[d] INRAE, UR RiverLy, centre de Lyon-Grenoble Auvergne-Rhône-Alpes, 69625 Villeurbanne Cedex, France
[e] Water Research Institute, National Research Council, 70132 Bari, Italy

ARTICLE INFO

Keywords:
Mediterranean catchments
Intermittent rivers
Hydrological regime
Suspended sediment transport

ABSTRACT

Flow and the sediment regime affect water quality and nutrient delivery in all river systems and are fundamental in sustaining the river ecosystem. This study aims to identify the most relevant factors affecting the flow regime and the suspended sediment transport in two Mediterranean intermittent rivers: the Búger (Spain) and the Carapelle (Italy). A set of hydrological indicators were used to characterize and classify the flow regime. High-resolution data, streamflow and suspended sediment concentration were used to quantify runoff and sediment yields at different temporal scales (annual, monthly, event). Rainfall, streamflow and sediment variables were used at the event scale to assess the rainfall-runoff-suspended sediment relationship through the Pearson correlation matrix. Hysteresis analysis provided information on sediment source dynamics. In the Búger River, the high degree of flow intermittence was mainly due to the presence of carbonate lithology and forest land use at headwaters promoting low values of runoff coefficient (2–10%) and specific suspended sediment yield (SSY; 0.5–46 t km^{-2} y^{-1}). In the Carapelle River, the high values of annual runoff coefficient (14–35%), together with low flow intermittence and SSY (89–745 t km^{-2} y^{-1}) were related to clay and flyschoid lithology. Most of the annual sediment yield (SY, t) was transported during floods. In Búger, SSY and maximum suspended sediment concentration ($SSC_{max,}$ g l^{-1}) were checked against runoff, peak discharge and antecedent rainfall. In Carapelle, SSY and SSC_{max} were checked against the amount and intensity of rainfall. The catchment size and the spatial distribution of rainfall, land uses and lithology played important roles in the flow regime, suspended sediment transport and hysteretic behaviour. Characterization of the flow regime linked to its main physical drivers improved understanding of the hydrological response and sediment transport variability of intermittent rivers. This study provided valuable insights into water resource management, improving the prediction of spatial patterns and of the intensity of sediment transport in river basins.

1. Introduction

The hydrological regime strongly affects water quality, nutrient and sediment delivery in all river systems (Wohl et al., 2015). The relevance of the flow regime is also recognized by river ecologists, who know that the dynamic variability of streamflow is fundamental to sustaining the ecological integrity of the river ecosystem (Poff et al., 1997). In addition, the Water Framework Directive (EC, 2000) –aiming at "good ecological status" for all waters– identified the hydrological and sediment regime as important factors in integrated river basin management (Prat et al., 2014).

Waterways that cease flow for some time of the year are defined as non-perennial rivers (Skoulikidis et al., 2017). Many definitions can be found in the literature of non-perennial waterways, mostly due to dry periods (i.e. temporary rivers, intermittent rivers, ephemeral streams, episodic streams; Datry et al., 2017). As a result, Datry et al. (2014) integrated these definitions in a new term: intermittent rivers and ephemeral streams (IRES), which may account for > 50% of the global

* Corresponding author.
E-mail address: giovanni.ricci@uniba.it (G.F. Ricci).

https://doi.org/10.1016/j.catena.2020.104865
Received 26 February 2020; Received in revised form 26 June 2020; Accepted 16 August 2020
Available online 09 September 2020
0341-8162/

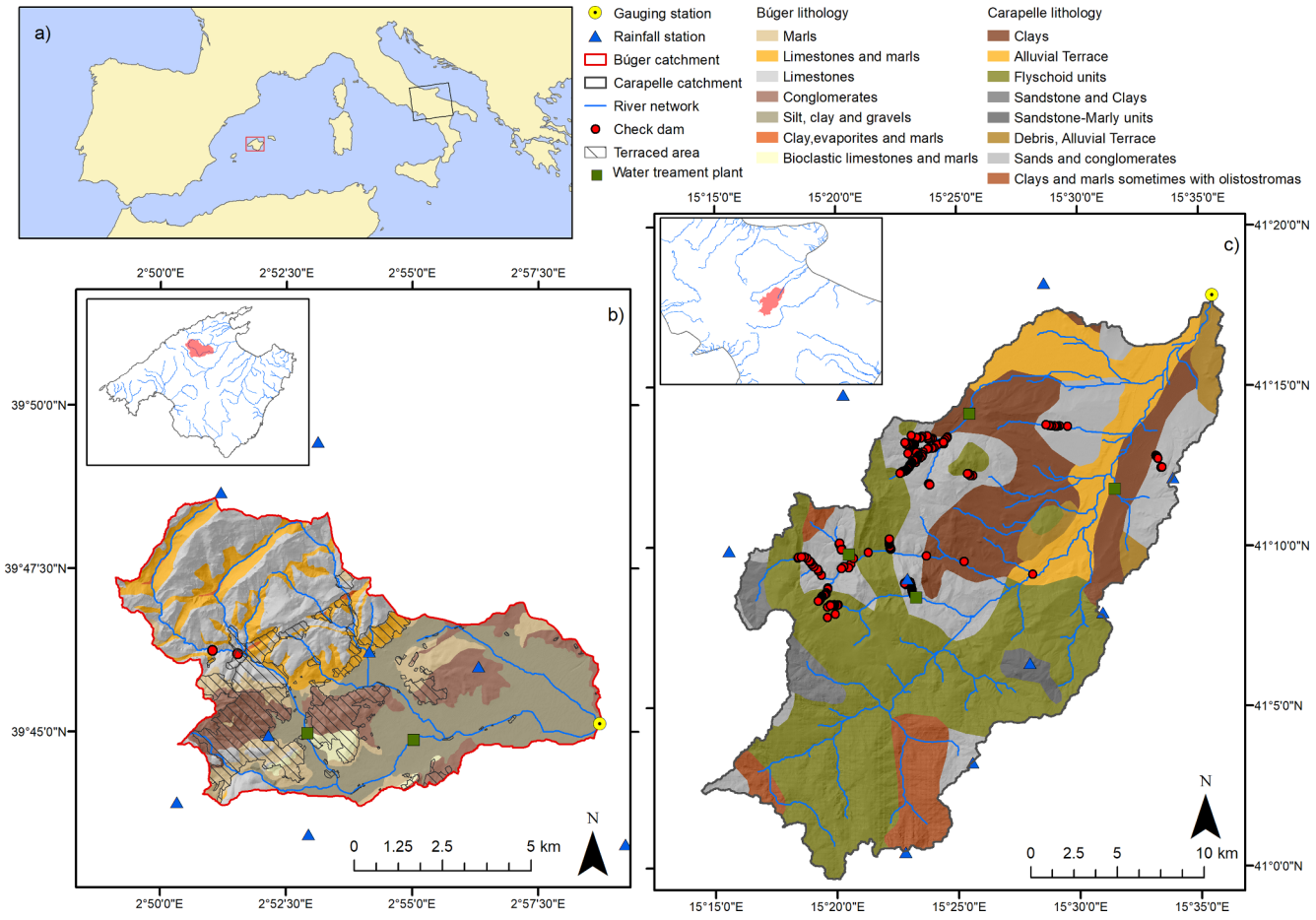

Fig. 1. Study area. (a) Catchments' geographical location in the Mediterranean area. Geographical location of (b) Búger and (c) Carapelle catchment with lithology, gauging stations, rainfall stations, check dams, water treatment plants, terraces and river network.

river network, including low-order streams. The degree of intermittence is expected to increase in the future across much of the world due to climate change and anthropogenic activities (Costigan et al., 2017; Sauquet et al., 2020, 2019). In IRES, the hydrological regime is the primary driving force controlling the sediment conveyance processes from upland to lowland catchment compartments, i.e. the river's geomorphology (Jaeger et al., 2017). Hydrological variability tends to be greater in IRES than in perennial rivers, due to specific and marked flow patterns in both wet and dry seasons. During the latter, streamflow gradually decreases until it disappears (Larned et al., 2010), whilst in the transition phase, sediment deposition within the channel is the main process but this is washed out regularly by flash floods (De Girolamo et al., 2015a; Estrany et al., 2011). In addition, as runoff generation processes are spatially heterogeneous and transmission losses are predominant (De Girolamo et al., 2015b), the sediment regime in IRES is different from than in perennial river systems.

Measurement of sediment transport enables us to understand fluvial dynamics better and characterize associated riverine processes governing water quality and habitats (Vericat and Batalla, 2006). In this context, sediment transport can be related to environmental impact in lowland areas and coastal zones (Berkun and Aras, 2012; Gamvroudis et al., 2015). However, the important role of the sediment regime in biodiversity, ecosystem functions and services, and its significance for river basin management, are rarely studied (Wohl et al., 2015). The main reason for this neglect of the sediment regime is the lack of data, a lack caused by the difficulty, expense and time required to measure sediment transport (Ricci et al., 2018). There are very few long-term measurements of sediment transport, especially in IRES. It is the key gap in our understanding of river sediment regimes (Bisantino et al., 2010; De Girolamo et al., 2018).

IRES studies have focused on the temporal and spatial variability of suspended sediment (SS) concentrations (García-Comendador et al., 2017; Vercruysse et al., 2017), on the drivers of SS transport (López-Tarazón and Estrany, 2017) or on evaluating reservoir siltation and the consequent loss of reservoirs' capacity for holding water (De Girolamo et al., 2018). Several studies have also analysed SS-discharge hysteresis during storm events within agricultural basins to identify dominant sediment sources and pathways (Gentile et al., 2010; Sherriff et al., 2016). However, the temporal and spatial dynamics of the hydrological regime have been generally neglected, especially for IRES (Acuña et al., 2014). It is essential to assess the relationships between sediment and runoff dynamics, if the sediment transport that is generated by soil erosion, a process identified as an environmental problem in the Mediterranean Region, is to be measure properly (Gamvroudis et al., 2015). Furthermore, limitations on hydrological models due to karstic features, global change effects and the lack of information about physiographic conditions mean that long-term hydrological data are required to assess flow and sediment regime in intermittent rivers (De Girolamo et al., 2015a; Skoulikidis et al., 2017).

This study analyses the hydrological regime and SS transport in the Búger and Carapelle catchments, located in Spain (Mallorca Island) and Italy (Apulia Region), respectively. Both are prone to flow intermittence. These basins, which share Mediterranean climate, have different physical features (i.e. catchment size, land use, soil, lithology). The complex interactions among these physical features are fundamental in influencing the flow regime and SS transport (Pagano et al., 2019). A set of hydrological indicators were used to characterize and classify the flow regime. High-resolution data, streamflow and

suspended sediment concentration were used for analysing floods. The sediment transport dynamics of the Carapelle have been investigated in part (García-Rama et al., 2016; Pagano et al., 2019): hydrological response and SS transport were assessed and compared at the event scale between Carapelle and an Alpine catchment. However, the analysis was not complete and SS transport was not measured at different time scales. The general objective of this study was to investigate the processes and the relationships between flow regime and SS transport in two streams under different degrees of flow intermittence. The specific objectives were to (a) quantify SS transport, (b) analyse the temporal variability of SS transport in response to the hydrological regime, and (c) identify the drivers of SS transport. The study contributes to better understanding of sediment transport dynamics in IRES in Mediterranean climate. It can be useful for water resources management, by predicting the spatial patterns and intensity of sediment transport in river basins.

2. Materials and methods

2.1. Study areas

The study areas are two Mediterranean catchments with intermittent river networks. The Búger catchment is located in the north of Mallorca (Spain, Fig. 1a), with its headwaters in the Tramuntana Range and the main course in the piedmont area known as Raiguer County. The Carapelle catchment is located in southern Italy, with its headwaters in the mountainous Dauno Sub-Apennine (Campania region) and the main course on the "Tavoliere delle Puglie" plain (Puglia region, Fig. 1a).

The Búger River (Fig. 1b) drains a catchment area of 68.2 km^2 at the gauging station. The altitude ranges from 55 to 1360 m a.s.l. with an average catchment slope of 31% (Fig. A.1a, Appendix A). The river is 21.6 km long with an average channel slope of 5% (13% in the first 7 km and 1% downstream). The lithology in lowland areas is alluvial, with clays and gravels (Fig. 1b). The catchment headwaters are characterized by massive limestone, marls and breccia (Table B1 Appendix B). Climate is classified as Mediterranean warm-summer (Csb) at headwaters and hot-summer in lowlands (Csa) on the Köppen climate classification (Kottek et al., 2006). Mean annual rainfall in lowland areas is 760 mm (1985–2006, Selva-Moscari AEMET station) and at the headwaters is 1201 mm (1985–2006, Lluc AEMET station). Rainstorms with a recurrence period of 2 years (headwaters) and 10 years (lowlands) may generate 100 mm of rainfall in 24 h (YACU, 2002). Agriculture is the main land use of the catchment: this is, mainly located in lowlands, while forest mostly covers mountain areas (Fig. A.1b Appendix A, Table B2 Appendix B). The main headwater subcatchment is regulated by the presence of check-dams constructed in the 1980 s. Traditional farm terraces occupy 20% of the catchment (i.e., 485 km of dry-stone walls). Furthermore, there are two water treatment plants at the villages of Selva (4014 inhabitants; INE, 2019) and Mancor de la Vall (1509 inhabitants; INE, 2019), which are located 6 and 10 km upstream of the hydrometric station (Fig. 1b). These plants spilled into the main channel during the period 2013–2017 an average monthly wastewater volume of 12,727 m^3 and 4267 m^3, respectively (GOIB, 2020).

The Carapelle River (Fig. 1c) drains a catchment area of 506 km^2 with a main channel length of 52.2 km that flows with an average channel slope of 1.8%. Altitude ranges between 120 m and 1089 m a.s.l and the average catchment slope is 16% (Fig. A.1c Appendix A). In the mountainous part of the catchment, the lithology (Fig. 1c) is mainly characterized by clayey-limestone and limestone-marly units which make up the flyschoid unit, while on the plain the main lithological classes are sands and conglomerates, clays and alluvial terraces (Table B1, Appendix B). The climate classification (Kottek et al., 2006) is Mediterranean, varying between warm (Cfa) at the headwaters and arid (Bsk) at the basin outlet. The mean rainfall at the headwaters is 778.9 mm (1921–2012, Bisaccia, Department of Civil Protection station) and 531.4 mm (1921–2012, Castelluccio dei Sauri, Department of Civil Protection station). The maximum 24 h-rainfall, with a recurrence period of 25 years, is about 110 mm day^{-1}. The Carapelle catchment is characterised by a strong presence of agricultural activities, occupying 79.5% of the catchment (Table B2, Appendix B), mainly winter wheat. In terms of area covered, forests follow agriculture (Fig. A.1d, Appendix A). In the mountainous areas of the Northern part of the catchment, many check-dams were built in the period 1960–1980 (Fig. 1c). There are four water treatment plants in the basin (17,302 inhabitants), which contribute with an average monthly wastewater volume of 105,180 m^3.

2.2. Data acquisition

Streamflow (Q) and suspended sediment concentration (SSC) were measured at the Búger gauging station near Búger village (39°45′7.548″N, 2°58′43.301″E) from 2013 to 2017. The water stage was continuously measured using a pressure sensor (Campbell CS451). Turbidity was recorded by a turbidimeter (OBS-3 + turbidimeter with a double measurement range of 0–1.000/1.000–4.000 NTU) connected to a Campbell Scientific CR200X data logger, which performs a 1 min reading and records an average value every 15 min. A rising-stage sampler modified from Schick (1967) was installed to provide more information on SSC. Water stage calibration, flow velocity measurements and stage-discharge rating curves were developed in line with the procedures of Fortesa et al. (2019). Water and SSC determination in samples were treated and used to calibrate turbidity records. Suspended sediment yields (SSY, t km^2 yr^{-1}) at annual, seasonal, monthly and event scales were calculated by combining the SSC and the Q. Daily and ten-minute rainfall data were obtained from AEMET-the Spanish Meteorological Agency (6 rainfall stations) and the MEDhyCON research group (2 rainfall stations).

Continuous measurements of Q and SSC were recorded from 2007 to 2011 at the Carapelle gauging station, located near the village of Ordona (41°17′50.347″N, 15°36′2.583″E) (Gentile et al., 2010). An electromechanical and ultrasound stage meter was used for Q measurements (Department of Civil Protection-National Hydrographic Service) and an infrared optical probe (Hach-Lange Solitax) was used for SSC. The probe was housed in a protection case to avoid the impact of flowing coarse material. The monitoring was controlled by a data acquisition set and a telemetry system for remote measurements was also provided. Both systems recorded data every 30 min. Daily Q data from 1970 to 2011 and daily and sub-daily (30-min) rainfall data were obtained from the Department of Civil Protection. Additional details about the instruments can be found in Gentile et al. (2010).

2.3. Hydrology and SS transport

The hydrological regime was characterized by means of a set of hydrological indicators (HIs; Richter et al., 1996). The selected HIs, computed on measured daily Q, proved to be relevant in IRES as pointed out by Oueslati et al. (2015), who classified temporary rivers in gauged Mediterranean catchments, and by D'Ambrosio et al. (2017), who characterized hydrological regime of gauged and ungauged intermittent rivers in Southern Italy. In-stream monitoring data (Q, SSC), were used to characterize the intra- and inter-annual variability of SSC and sediment yield.

2.3.1. Annual and monthly analysis

The flow regime was classified in relation to the degree of intermittence, the long-term mean annual relative number of months with flow (Mf; Arscott et al., 2010) and the 6-month seasonal predictability of the dry period (Sd6, Eq. (1); Gallart et al., 2012). Both HIs were also used as coordinates in a plot, in order to classify the streams visually on the basis of their degree of intermittence.

$$Sd6 = 1 - \frac{\sum_1^6 Fdi}{\sum_1^6 Fdj} \quad (1)$$

where *Fdi* is the multi-annual frequencies of zero-flow months for the contiguous six wetter months of the year and *Fdj* is the multi-annual frequencies of zero-flow months for the remaining six drier months.

This classification divides the river regime, and thus the river types (Gallart et al., 2012), in four classes: perennial (P), intermittent-pools (I-P) (in dry season, only subsurface flow occurs), intermittent-dry (I-D) (surface and subsurface flow are absent for at least 1 month a year) and episodic-ephemeral (E) (water flow and pools are occasional). The present study classified the Carapelle River with daily Q data from 1970 to 2011; and data and the Búger catchment, with data from 2013 to 2017.

Flow magnitude was described through the median annual runoff (R_a; mm), the runoff (R; mm) for each month and the groundwater or subsurface contribution to Q, the baseflow index (BFI). The BFI was calculated as the ratio of the annual baseflow to the total annual flow. In ephemeral streams, the BFI may be close to 0, whereas in catchments with high groundwater contributions the BFI is close to 1 (Smakhtin, 2001). The Richards-Baker Flashiness Index (FI, Eq. (2)) (Baker et al., 2004) was used to calculate the rate of changes in Q. The median of the annual values was taken as the representative value.

$$\sum \mathrm{FI} = \frac{\sum qi - qi_{-1}}{\sum qi}\mathrm{qi} \quad (2)$$

where *qi* is the daily Q at the time *i*, and qi_{-1} is the daily Q at the time i_{-1}.

The maximum annual flow of 1-day duration (DH1), and the number of days without flow (number of zero-flow days, DL6) were analysed to describe extreme flow conditions. Finally, the timing of maximum and minimum flows was computed (TH1, TL1).

The temporal variability of SY was analysed for both streams. Annual and median monthly specific SY (SSY, t km^{-2}) were estimated over the study period. Magnitude and timing of extreme sediment transport conditions were calculated and a flashiness index for sediment (the Sediment Flashiness Index; SFI) was computed to calculate the rate of change in the SY in order to evaluate the response of sediment transport to the streamflow. The SFI was calculated using Eq. (2), where daily SY was used instead of daily Q.

Flow duration curves (FDC) were also developed for specific R and SSY per unit area by using data measured at the gauging stations. The FDCs and sediment duration curves (SDCs) graphically characterize the time during which a specified flow or SSY is equalled or exceeded (Kannan et al., 2018).

2.3.2. Event scale analysis

A number of floods were selected on the FDC by using a distribution frequency of 95%. The beginning of floods was identified as the time that showed a significant increase in Q; while the end was taken as the breakpoint of the recession limb (Custodio and Llamas, 2005). Moreover, flood events after the dry period were added to this analysis due to their relevance during the storage and release periods of SS in IRES (De Girolamo et al., 2015ab; Vercruysse et al., 2017). Events in which sediment data were missing (particularly in 2009 for Carapelle and in 2015 for Búger) were discarded, since a complete analysis was not possible. As a result, 25 and 23 events were selected for the Búger and Carapelle rivers, respectively. Flood events were analysed by 12 variables divided into three groups: rainfall, R and sediment variables (Table 1). The relationships between rainfall, R and SS transport variables were assessed through a Pearson correlation matrix using the statistical SPSS software.

According to Baker et al. (2004), the flashiness index equation (Eq. (2)) was adapted to the sub-daily data as indicated in the following equation (Eq. (3)):

$$\mathrm{FI} = \frac{\sum |qhri - qhri_{-1}|}{\sum qi} \quad (3)$$

where *qhri* is the sub-daily Q at time *i* (15-min for the Búger and 30-min for the Carapelle).

SFI was also calculated for the events analysed by the SSY in Eq. (3).

The relationship between Q and SSC was investigated by means of the hysteresis analysis reported by Williams (1989). Hysteretic loops are classified as linear when Q and SSC peaks (Q_{max} and SSC_{max}) occur at the same time; the clockwise loop when SSC_{max} occurs earlier than Q_{max}; and counter-clockwise loop when Q_{max} occurs later than SSC_{max}. Clockwise and counter-clockwise loops are circular in case of single peaks, while multiple peaks of Q or SSC create a combination of these loops that are called eight-shaped.

3. Results

3.1. Classifying streamflow regime

The time during which a specific flow or SSY is equalled or exceeded is represented as a percentage in Fig. 2 through the FDC and SDC on a daily time scale. The flow permanence observed at the Búger River gauging station was < 30% of the time. The FDC assumed a very sharp shape in extremely high flows (0–2% exc. freq.), in high flows (2–5% exc. freq.), and also in normal and low-flow conditions, demonstrating a rapid response in both the rising and recession phase. From extreme-high flow to high flows (0–5% exc. freq.) specific R ranged from 0.23 to 0.003 mm km^{-2}.

The FDC of Carapelle is characterized by a steep slope in extreme-high flow (0–5% exc. freq.). In high flow (5–20% exc. freq.) and normal flow, a gentle slope was observed. A few days without flow were recorded from 2007 to 2011. The specific R ranged from 16.07 to 5.03 mm km^{-2} in extremely high flow and decreased rapidly in the high flow phase, reaching 0.69 mm km^{-2}. In normal flow (20% of exc. freq.), specific R was between 0.69 and 0.07 mm km^{-2}.

The SDC was matched with the FDC in the Búger River. The SDC showed a sharp decrease in the FDC for extreme-high flow (0–2% of exc. freq.) and high flow conditions (2–5% of exc. freq.). Specific SSY ranged from 32.1 to 0.03 t km^{-2} day^{-1} and 0.03 to 0.007 t km^{-2} day^{-1}, respectively. During normal flow conditions (5–22% exc. freq.) low values of SSY, ranging from 0.007 to 0.0004 t km^{-2} day^{-1}, were seen. The SSY contribution during extreme-high flows and high flows represented the 97% and 1.3% of the total SSY, respectively.

The SDC for the Carapelle River showed a rapid decrease in SSY for extreme-high flow conditions, ranging from 304 to 3.78 t km^{-2} day^{-1}. A prompt decrease from 3.78 to 0.21 t km^{-2} day^{-1} was also recorded in high flow. Under normal flow conditions, SSY was between 0.21 and 0.025 t km^{-2} day^{-1}. The contributions to total SSY in extreme high flow and high flow conditions were 90% and 7%, respectively, whilst this contribution to total SSY under low flow conditions was 0.15%.

By using the metrics Sd6 and Mf as coordinates in the plot reported in Fig. 3, the Búger and Carapelle rivers were classified in average conditions as an I-D and I-P stream, respectively. In the study period, the Búger ranged between I-P and E and the Carapelle from P to I-P.

3.2. Analysing hydrology and sediment transport

The hydrological parameters, SSY and the selected HIs calculated on a yearly basis, are summarized in Table 2. The pattern of daily rainfall (mm), Q (m^3 s^{-1}) and SSC (g l^{-1}) recorded on the daily time scale are analysed and reported in Fig. 4(a, b).

In both catchments, rainfall and hydrological regimes were characterized by a wet and a dry season. Both the annual rainfall amount and the number of high rainfall events (> 25 mm) recorded in the Búger catchment were higher than in the Carapelle. On the contrary, the runoff coefficient (3%, ranging from 2 to 10%) in the Búger was

Table 1
Rainfall, runoff and sediment variables considered in the event scale analysis.

Rainfall variables		Runoff variables		Sediment variables	
P_{tot}	Total precipitation (mm)	Q_{dur}	Flood duration (h)	SSC_{max}	Max. susp. sed. conc. (g l^{-1})
$IP_{max}30$	Max. 30′ prec. intensity (mm h)	Q_{max}	Max. discharge (m^3 s^{-1})	SFI	Sediment flashiness Index
AP1d	Antec. Prec. 1 day before (mm)	Q_0	Discharge at time 0 (m^3 s^{-1})	SSY	Specific sediment yield (t km^{-2})
AP3d	Antec. Prec. 3 day before (mm)	FI	Flashiness Index		
		R	Runoff (mm)		
		R_c	Runoff coefficient (%)		

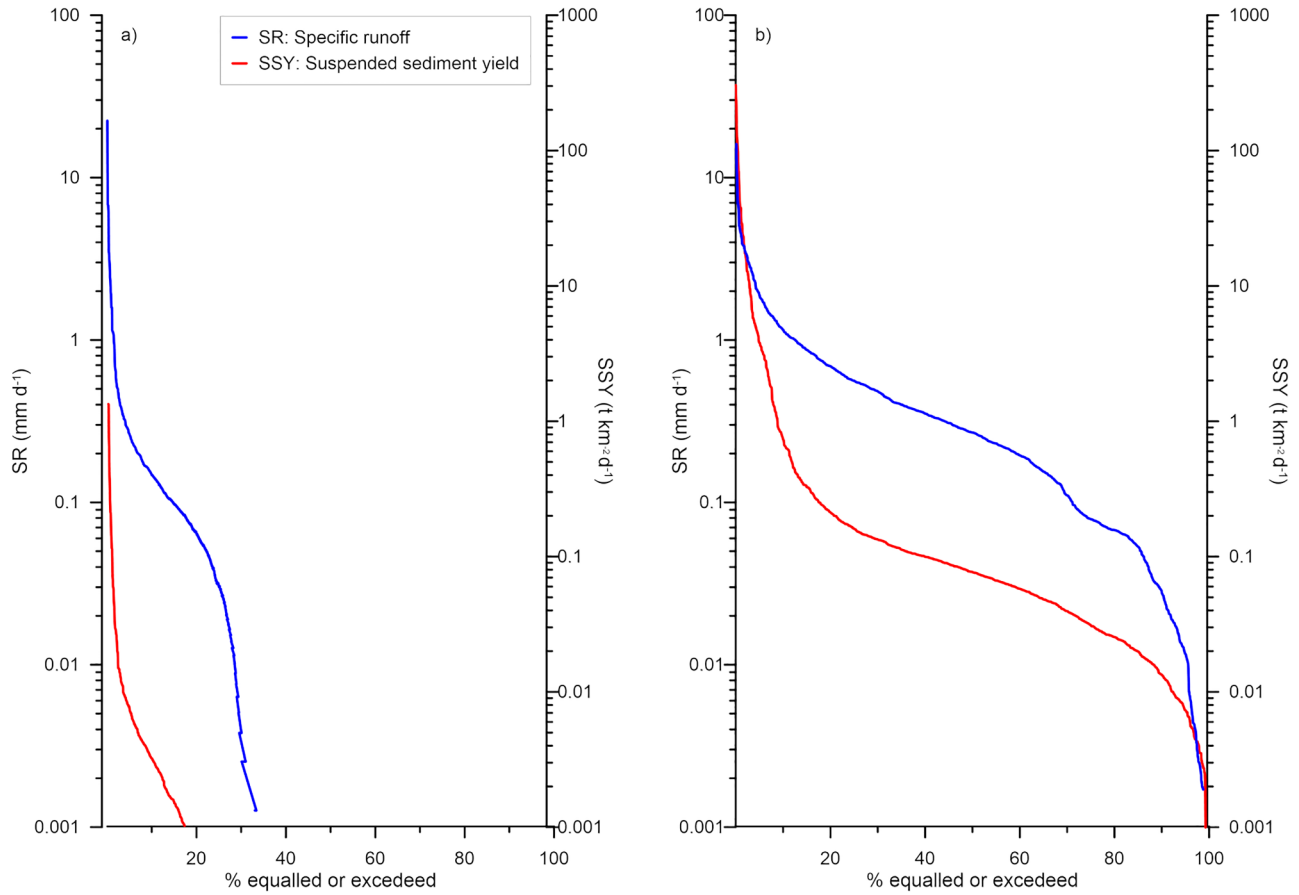

Fig. 2. Specific runoff (blue line) and specific suspended sediment yield (red line) duration curves at (a) Búger and (b) Carapelle Rivers based on daily values. (For interpretation of the references to colour in this figure legend, the reader is referred to the web version of this article.)

lower than in the Carapelle (16%, ranging from 14 to 35%) (Table 2). Streamflow in the Carapelle was higher than in the Búger catchment. The hydrographs of both rivers are characterized by steep rising and recession limbs, although the latter is less accentuated in the Carapelle (Fig. 4a, b). The R_a contribution was 25.38 mm (from 11.38 mm to 91.11 mm) in the Búger and 90.6 mm (from 75.0 mm to 307.8 mm) in the Carapelle (Table 2).

Seasonal rainfall patterns can be seen on a monthly scale in the Búger (Fig. 5a), where the rainiest months (November to January) reached 300 mm. On the contrary, monthly rainfall was $<$ 100 mm from mid-spring to early autumn (May to October). In the Carapelle (Fig. 5b), the rainiest months were from autumn to the beginning of spring; the maximum monthly amounts (i.e., 170 mm) were lower than in the Búger. The lowest monthly rainfall amounts were recorded in July and August in the Búger and Carapelle, respectively (i.e. $<$ 50 mm).

The wet season generally ran from November to May in the Búger catchment, with 84% of the R_a in three months: January (46%), February (19%) and December (19%) (Fig. 5c). In the dry season, flash flood events occurred, except in July and August. The Carapelle river was characterized by a longer wet season (October to June; R $>$ 5 mm) (Fig. 4b) with a monthly R ranging from 4.8 mm to 66.5 mm (Fig. 5d). The major R contributions were recorded in March (21%), January (17%) and April (15%). The dry season, from July to September, was characterized by an average monthly R $<$ 5 mm.

As Table 2 shows, the median annual BFI was 0.45 (from 0.30 to 0.59) and 0.54 (0.36–0.58) in the Búger and Carapelle, respectively. Higher inter-annual variability in the rate of changes in streamflow was recorded in the Búger, where FI ranged from 0.22 to 0.76 as against 0.31–0.56 in the Carapelle River. While DH1 reached four orders of magnitude in the Búger, it had a higher value and less variability in the Carapelle River. In both study areas, the period of high flow was generally from December to April (TH1 varies from 315 to 120, see Table 2). Extreme low flow conditions occurred mainly between early spring to early autumn, with TL1 ranging from 112 to 153 in the Búger, with the median DL6 of 237. Very few low number of DL6 was recorded during 4 years of measurements in the Carapelle (from 0 to 54 days).

In the Búger, SY was limited to a few events (R $>$ 20 mm), which

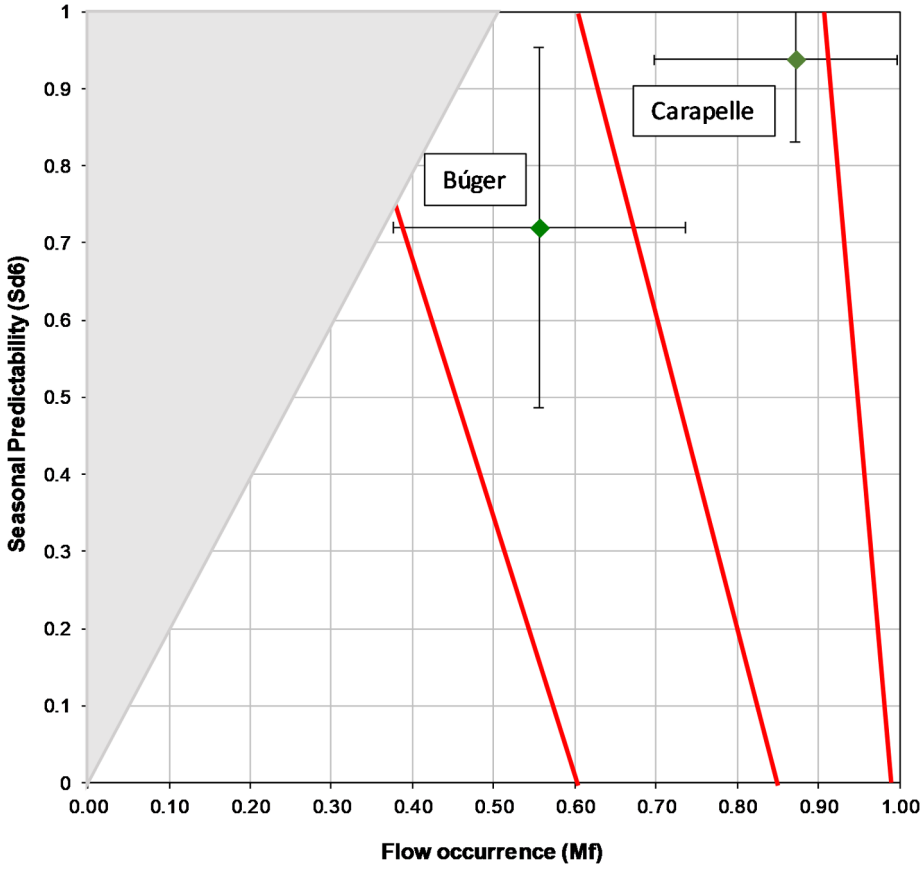

Fig. 3. River regime by flow permanence (Mf) and six-month seasonal predictability of dry period (Sd6) (Gallart et al., 2012). Red lines stand for the separation between the different regime types. The grey triangle shows the area where the metrics are incompatible. Bars show the standard errors. Flow regime acronyms: (E) episodic-ephemeral, (I-D) intermittent-dry, (I-P) intermittent-pools and (P) perennial. (For interpretation of the references to colour in this figure legend, the reader is referred to the web version of this article.)

accounted for almost the total annual SY of the catchment. The magnitude of the Q was between 0 and 17.9 $m^3\ s^{-1}$ and the SSC ranged between 0 and 1.2 g l^{-1} (Fig. 4a). The largest flood occurring in the Búger during the study period generated a runoff of 23.6 mm and a SSY of 35.5 t km^{-2} with a rainfall amount of 55.7 mm. The Carapelle River was characterized by a higher SY caused by R events lower than 20 mm. Indeed, Q ranged between 0 and 94.1 $m^3\ s^{-1}$ and SSC varied between 0.01 and 35.6 g l^{-1} (Fig. 4b). The largest flood, recorded on 10th November 2010, generated a runoff of 18.2 mm and a SSY of 303 t km^{-2} with a rainfall amount of 14.4 mm.

SSY was matched with R and showed high variability in both basins. The median annual SSY in the Búger catchment was 1.51 t $km^{-2}\ y^{-1}$, which was lower than in the Carapelle (267.78 t $km^{-2}\ y^{-1}$). Analogous behaviour was found in the rate of change of SSY, where differences of up to two and three orders of magnitude are shown in the Carapelle and Búger respectively (Table 2).

Fig. 5e shows the monthly SSY for both basins. In the Búger catchment, most annual SSY was delivered in January (87.0%),

Table 2
Annual rainfall, Annual runoff (R_a), runoff coefficient (R_c), Zero-day flow (DL6), Specific Sediment Yield (SSY), Base Flow Index (BFI), Flashiness index (FI), Sediment Flashiness Index (SFI) and HI for the Búger and Carapelle catchments.

	Búger										
Year	Rainfall (mm)	R_a(mm)	R_c (%)	DL6	SSY (t $km^{-2}\ yr^{-1}$)	BFI	FI	SFI	DH1	TH1	TL1
2013	1019.35	26.86	3	204	0.79	0.44	0.22	0.36	0.23	120	153
2014	719.10	11.38	2	237	0.49	0.55	0.76	0.92	1.26	356	133
2015	606.30	25.38	4	212	1.51	0.59	0.51	0.60	2.76	36	153
2016	867.88	16.73	2	329	3.92	0.30	0.48	0.52	0.058	46	140
2017	870.20	91.11	10	250	45.97	0.45	0.25	0.38	17.68	21	112
Median 2013–17	867.88	25.38	3	237	1.51	0.45	0.48	0.52	1.26		
	Carapelle										
Year	Rainfall (mm)	R_a (mm)	R_c (%)	DL6	SSY (t $km^{-2}\ yr^{-1}$)	BFI	FI	SFI	DH1	TH1	TL1
2007	542.01	75.00	14	0	89.31	0.56	0.45	1.53	38.93	96	268
2008	546.00	93.50	17	54	123.70	0.58	0.31	1.44	20.25	67	193
2009**	785.74	–	–	–	–	–	–	–	–	–	–
2010	888.98	307.80	35	4	745.40	0.52	0.49	1.17	94.09	315	206
2011	546.04	87.70	16	1	411.86	0.36	0.56	1.31	67.46	65	262
Median 2007–11	546.04	90.60	16	2.5	267.78	0.54	0.47	1.38	53.19		

** The year 2009 was not included in this table due to the lack of data on both runoff and sediment load (maintenance of the gauging station).

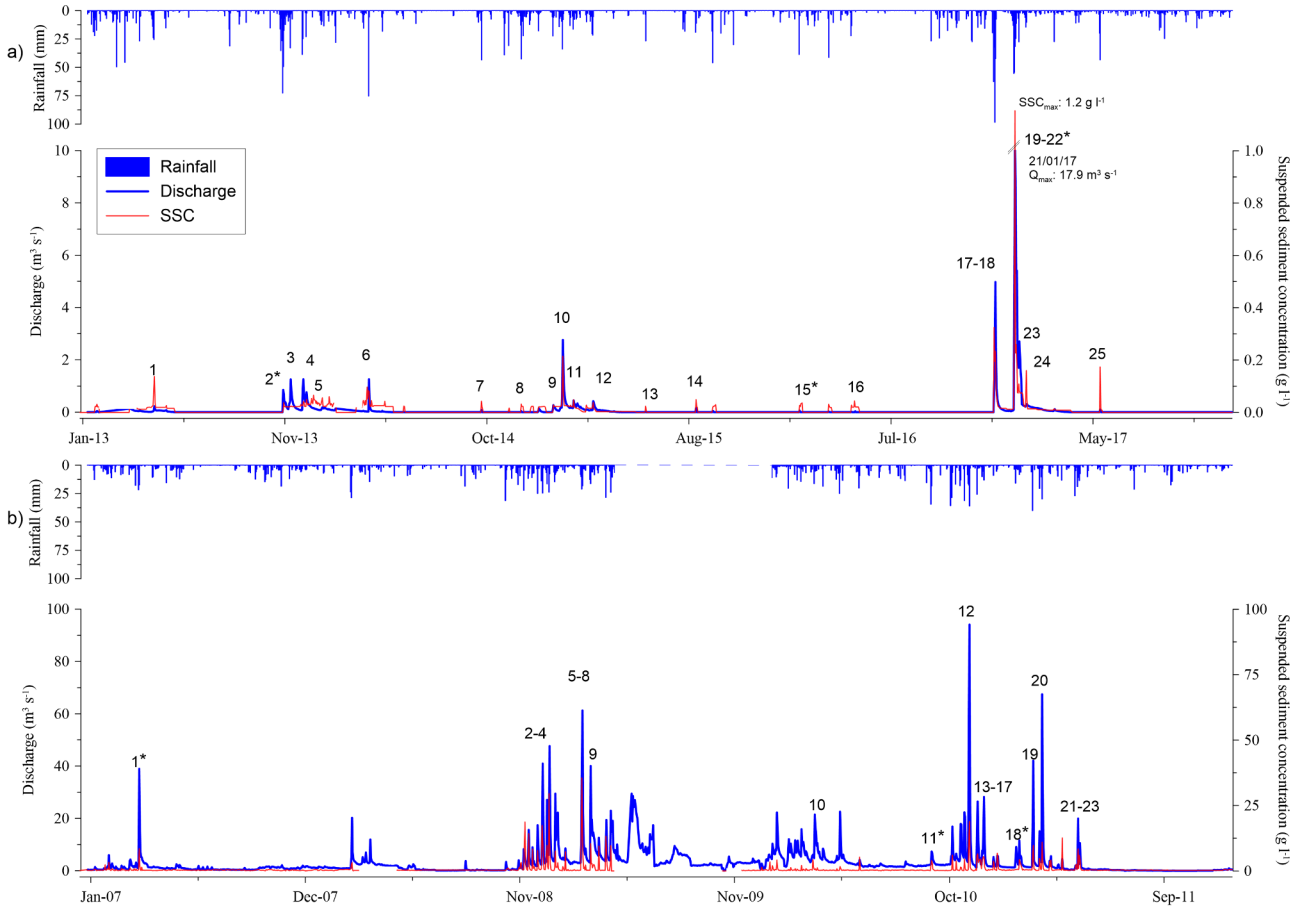

Fig. 4. Streamflow and SSC on a daily time scale: (a) Búger and (b) Carapelle Rivers. The numbers located at the peak of each hydrograph indicate the ID of the events recorded during the study period. Selected events for the hysteresis analysis are denoted with the asterisk (*).

December (8.3%) and February (3.1%), when monthly R runoff was high; whilst the SSY was very low in the rest of the year. In the Carapelle catchment, the SSY was recorded throughout the year, with the largest values (i.e. SSY > 100 t km^{-2}) recorded in November (40.6% of annual amount), March (16.5%) and December (13.6%) (Fig. 5f).

3.3. Variability at the event scale

Rainfall, runoff and sediment variables calculated at sub-daily time steps (15-min and 30-min for the Búger and Carapelle, respectively) for the selected flood events are summarized in Tables 3 and 4. The R and

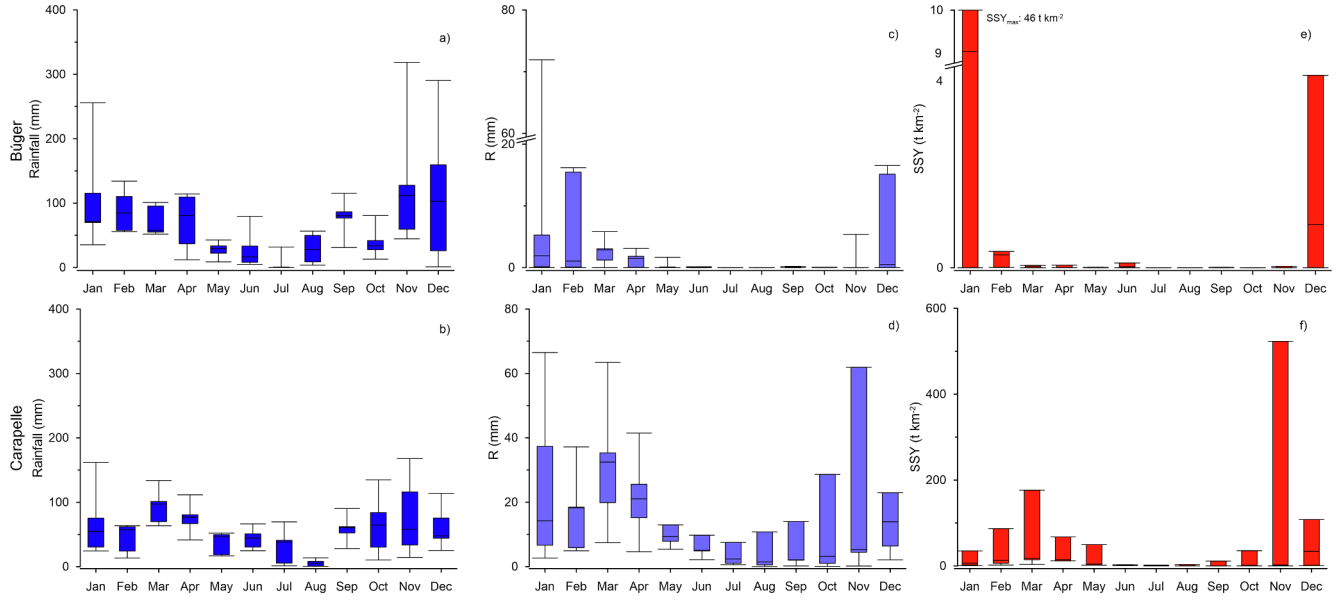

Fig. 5. Box plots show the minimum, median and maximum monthly rainfall, runoff (R) and specific suspended sediment yield (SSY) contributions of the Búger (a, c and e) and Carapelle (b, d and f) catchment.

Table 3
Factors calculated at the 15-min time step for the flood events selected for the Búger catchment. The hysteresis direction (Hyst. dir.) and the hysteresis shape (Hyst. shape) are described as C: clockwise; CC: counter-clockwise; C: circular; E-S: eight-shaped.

ID	Date	P_{tot} (mm)	$IP_{max}30$ (mm h^{-1})	AP1d (mm)	AP3d (mm)	Q_{dur} (h)	Q_0 (m^3 s^{-1})	Q_{max} (m^3 s^{-1})	FI	R (mm)	R_c (%)	SSC_{max} (g l^{-1})	SFI	SSY (t km^{-2})	Hyst. Dir.	Hyst. Shp
1	28/04/13	23.0	4.0	24.0	45.3	42.8	0.0	0.34	0.02	0.4	1.7	0.24	0.05	0.05	C	E-S
2	19/11/13	99.7	18.0	6.6	60.4	14.8	0.0	1.96	0.07	0.9	0.9	0.15	0.15	0.05	CC	E-S
3	01/12/13	35.9	7.4	5.1	20.3	53.0	0.4	1.85	0.01	2.8	7.8	0.04	0.02	0.07	C	C
4	20/12/13	62.7	7.0	5.7	5.7	52.3	0.1	1.93	0.01	3.7	5.9	0.08	0.07	0.12	C	C
5	26/12/13	22.9	6.0	2.0	2.0	50.5	0.4	0.99	0.01	1.6	7.0	0.15	0.20	0.08	CC	C
6	04/04/14	76.0	9.0	0.2	0.2	14.0	0.0	4.33	0.08	1.3	1.8	0.30	0.24	0.13	C	C
7	29/09/14	43.5	17.9	8.8	10.1	3.8	0.0	1.21	0.29	0.1	0.2	0.29	0.38	0.01	C	C
8	01/12/14	41.8	17.8	1.3	6.7	11.0	0.0	0.29	0.17	0.0	0.1	0.23	0.20	0.00	CC	C
9	20/01/15	28.2	12.0	5.5	7.1	33.3	0.0	0.45	0.02	0.5	1.7	0.09	0.09	0.01	C	C
10	04/02/15	46.3	8.4	9.5	15.8	58.3	0.2	3.31	0.01	6.2	13.4	0.63	0.06	1.11	C	C
11	22/02/15	26.9	5.2	5.0	0.0	38.8	0.1	0.58	0.01	0.8	2.9	0.16	0.08	0.03	C	C
12	25/03/15	27.0	6.3	20.4	28.1	53.0	0.1	0.50	0.01	1.1	4.1	0.07	0.04	0.04	C	E-S
13	16/06/15	26.8	20.6	3.2	3.2	6.0	0.0	0.17	0.52	0.0	0.0	0.18	0.77	0.00	CC	E-S
14	04/09/15	19.1	ND	0.5	2.1	8.8	0.0	2.09	0.28	0.2	1.0	0.19	0.33	0.03	C	E-S
15	15/02/16	38.7	14.8	0.8	1.6	5.5	0.0	0.37	0.15	0.1	0.2	0.29	0.48	0.01	C	C
16	13/05/16	7.4	ND	0.0	0.1	4.3	0.0	0.41	0.39	0.0	0.5	0.29	0.43	0.01	C	C
17	19/12/16	76.1	3.8	0.2	19.8	13.5	0.2	2.50	0.06	1.0	1.3	2.40	0.19	0.75	CC	E-S
18	20/12/16	145.7	13.8	32.4	94.9	66.8	0.3	6.36	0.02	11.6	8.0	1.44	0.09	3.00	C	C
19	20/01/17	77.6	10.9	27.6	40.8	25.3	0.2	8.12	0.03	7.3	9.5	1.81	0.08	3.35	C	C
20	21/01/17	55.7	7.8	33.1	80.2	23.8	5.0	49.93	0.05	23.6	42.4	6.31	0.30	35.45	C	E-S
21	24/01/17	23.0	4.1	23.9	53.8	25.8	4.0	8.22	0.01	8.0	35.0	1.01	0.16	2.29	C	E-S
22	27/01/17	27.6	7.2	6.9	10.8	24.5	1.4	3.46	0.01	3.5	12.5	0.19	0.03	0.41	C	C
23	08/02/17	24.9	7.5	6.1	11.1	19.5	0.4	1.90	0.02	1.4	5.6	0.50	0.10	0.26	CC	E-S
24	24/03/17	27.6	4.6	1.5	1.5	29.0	0.0	0.25	0.03	0.2	0.7	0.03	0.06	0.00	C	E-S
25	05/06/17	60.1	20.4	3.4	6.6	6.5	0.0	0.48	0.11	0.1	0.2	3.24	0.41	0.10	CC	C

Table 4
Factors calculated at 30-min time steps for the flood events selected in the Carapelle catchment. The hysteresis direction (Hyst. dir.) and the hysteresis shape (Hyst. shape) are described as C: clockwise; CC: counter-clockwise; C: circular; E-S: eight-shaped; L: linear.

ID	Date	P_{tot} (mm)	$IP_{max}30$ (mm h^{-1})	AP1d (mm)	AP3d (mm)	Q_{dur} (h)	Q_{max} (m^3 s^{-1})	Q_0 (m^3 s^{-1})	FI	R (mm)	R_c (%)	SSC_{max} (g l^{-1})	SFI	SSY (t km^{-2})	Hyst. Dir.	Hyst. Shp
1	05/04/07	24.76	2.09	19.34	19.43	46.50	63.85	5.83	0.05	9.32	37.65	21.66	0.14	76.09	C	E-S
2	11/12/08	8.21	2.08	13.85	14.25	8.00	39.16	1.83	0.17	1.33	16.14	62.94	0.38	44.88	CC	E-S
3	12/12/08	2.44	0.68	24.56	25.18	14.50	33.16	8.50	0.09	1.95	79.90	19.44	0.19	21.45	CC	C
4	26/12/08	10.87	0.79	11.96	11.96	24.00	39.73	2.52	0.07	3.96	36.47	17.59	0.12	45.27	CC	C
5	06/03/09	0.43	0.15	21.07	23.41	7.50	37.47	14.33	0.10	1.67	383.08	59.75	0.24	52.68	CC	C
6	06/03/09	10.98	1.05	11.04	29.06	39.00	119.40	10.63	0.09	16.34	148.85	43.93	0.16	348.76	CC	E-S
7	20/03/09	5.64	0.85	21.70	21.79	19.00	70.61	21.86	0.08	5.66	100.37	21.03	0.14	73.09	C	E-S
8	22/03/09	4.29	0.34	3.68	29.35	29.50	29.61	12.40	0.02	3.90	90.96	6.52	0.09	11.86	CC	C
9	26/03/09	1.54	0.49	5.59	20.93	12.50	19.82	9.53	0.07	1.21	78.38	6.64	0.15	4.08	CC	C
10	14/03/10	1.31	0.20	3.01	10.41	23.50	14.66	8.75	0.03	1.79	136.61	3.34	0.11	2.20	CC	C
11	11/09/10	0.35	0.28	34.49	56.65	16.00	20.62	2.97	0.08	1.38	388.33	15.24	0.19	8.82	CC	C
12	10/11/10	14.41	2.90	18.64	43.28	31.00	153.74	48.80	0.05	18.15	125.98	42.34	0.16	242.07	C	E-S
13	22/11/10	5.74	1.71	19.12	19.52	11.50	58.84	1.38	0.14	2.62	45.56	27.81	0.26	41.08	C	E-S
14	23/11/10	3.21	0.70	26.50	27.00	13.00	55.39	14.66	0.08	3.25	101.13	11.14	0.00	27.84	CC	E-S
15	24/11/10	0.14	0.08	4.36	33.06	14.50	17.51	8.26	0.06	1.23	877.35	5.40	0.06	4.16	CC	C
16	02/12/10	0.65	0.31	4.70	17.97	8.50	33.68	3.92	0.15	1.17	180.63	18.85	0.24	13.52	CC	C
17	03/12/10	2.19	0.33	14.51	24.49	14.50	72.16	4.72	0.09	4.36	199.09	21.03	0.22	39.93	C	E-S
18	28/01/11	3.51	0.39	8.79	13.20	25.50	25.81	2.74	0.07	2.27	64.68	14.20	0.13	15.75	CC	C
19	19/02/11	13.88	3.27	27.53	34.89	15.00	159.50	1.70	0.12	8.28	59.67	37.36	0.22	213.76	C	L
20	01/03/11	6.71	0.90	16.24	21.81	14.50	59.55	1.67	0.14	2.62	39.01	23.48	0.30	26.98	CC	C
21	01/05/11	18.35	1.62	13.63	18.06	31.50	42.65	0.97	0.08	3.67	19.97	23.33	0.19	36.15	CC	C
22	03/05/11	3.02	0.75	11.47	43.44	13.50	34.21	1.98	0.15	1.43	47.31	20.26	0.24	16.73	CC	C
23	04/05/11	5.22	0.51	14.68	30.86	17.50	24.45	5.83	0.09	1.62	31.01	18.75	0.20	10.25	CC	C

SSY contributions recorded in the selected events were 48% and 90% of the annual amount in the Búger; and 14% and 80% in the Carapelle, respectively. In the Búger, the largest event (Table 3) generated an R of 25.0 mm and an SSY of 35.45 t km^{-2} (Q_{dur}: 24 h), which were 27% and 77% of the R and the SSY recorded during 2017. In the Carapelle, however, during the largest event in terms of R (18.15 mm), a SY of 242.07 t km^{-2} was recorded (Q_{dur}: 31 h, Table 4). The contributions of R and SSY for 2010 was 6% and 32% respectively.

A wide range of runoff response and sediment transport was found in the two study areas. The variables controlling hydrological response seem to be different between basins. Analysis of the rainfall variables make clear that the threshold of rainfall needed to generate runoff is different in the two basins. As Table 3 shows, P_{tot} and $IP_{max}30$ were higher in the Búger catchment than in the Carapelle. This was expected, as both the infiltration capacity of soil and the lithology of the two basins differ.

The pre-event rain (rain recorded before flood), which was analysed here through the precipitation recorded 1 day before the event (AP1d) and 3 days before it (AP3d), and Q at time 0 (Q_0) seem to be the main factors contributing to the streamflow in the Búger catchment. Indeed, as Table 5 shows, there was a strong correlation between pre-event variables (AP1d, AP3d and Q_0) and Q_{max}, R and R_c.

In the Carapelle, Q_{max} and R correlated with P_{tot}, $IP_{max}30$ and Q_0, whilst AP1d and AP3d did not correlate with any variable (Table 6). This is probably because rainfall events are generally localized in small areas, which means that use of the Thiessen polygons to calculate mean precipitation in a large drainage area misses some relevant information such as the correlation with floods. The median value of flood duration, Q_{dur}, was about 20 h in both basins, although in the Búger greater standard deviation was found.

Both catchments showed a non-linear relationship between rainfall and runoff. In the Búger, rainfall events of 60 mm may generate a runoff response from 0.1 to 25 mm, depending on the season and the antecedent precipitation of the runoff event (Table 5). This variability was also seen in the Carapelle catchment, where rainfall events close to 15 mm generated a runoff response from 4 to 18 mm (Table 6). In both catchments the FI had strong positive correlation with SFI and strong negative correlation with Q_{dur}. Furthermore, in the Búger the FI also correlated with $IP_{max}30$.

Rainfall variables depicted difference in sediment transport between the basins. In Búger AP1d and AP3d correlated with SSC_{max} and SSY. These sediment variables correlated strongly with Q_0, Q_{max}, R and R_c. In the Carapelle, P_{tot} and $IP_{max}30$ were correlated with the SSY, with the correlation with rainfall intensities being more significant. $IP_{max}30$ also correlated with the SSC_{max}, which also correlated with Q_{max} and the FI. Closer correlations ($p < 0.01$) were observed between SY and Q_{max} and R. In both catchments SSC_{max} depicted close correlation with SSY. In the Búger, higher contributions of the SSY were found in those events with $SSC_{max} > 1$ g l^{-1}, most of which were in autumn or winter. In the Carapelle, the highest contributions of the SSY were seen when $SSC_{max} > 30$ g l^{-1}, events generally occurring in autumn and winter.

Different hysteretic loops were observed in the two basins. For the 25 analysed flood events in the Búger, predominantly clockwise hysteresis behaviour (72%) was found (Table 3). Among these 67% were circular while 33% were eight-shaped. Events with clockwise hysteresis generated 93% of the total R and 97% of the total SY. In the Carapelle, however, the prevalent hysteresis loops (74%) were counter-clockwise (Table 4). In particular, 82% were circular and 18% were eight-shaped. In these kinds of events, the R contribution was 51% while the SY contribution was 49% of total recorded amounts. Differences were seen for the Carapelle in the largest floods, which had a predominantly clockwise hysteresis loop.

Fig. 6 reports some hysteresis loops (events after dry period, $Q > 95\%$). In both catchments, the hysteresis in events after dry period and $Q > 98\%$ were counter-clock and clockwise, respectively, showing eight-shaped loops in multi-peak events. Besides, in events after dry period and $Q > 95\%$ the SSC_{max} values were similar in each catchment. However, in $Q > 98\%$ evens, the largest values of Q and SSC_{max} were found in both catchments, being in Búger SSC_{max} one order of magnitude higher than events after dry period and $Q > 95\%$.

4. Discussion

Hydrological regimes are clearly influenced by fluctuations in the groundwater table and the nature of the flow pathways into and out of the river channel, exerting controls on sediment transport (Sear et al., 1999). Disentangling these control mechanisms in IRES is a crucial issue because the number and length of intermittent rivers in regions that experience drying trends are likely to increase under global change scenarios (Larned et al., 2010). This paper analyses hydrology and sediment transport in two IRES in Mediterranean environments. Soil permeability, lithology and geological features were the most relevant factors affecting the flow regime and the intermittence of the rivers, while climate had a minor influence. Indeed, although the mean annual rainfall was higher in Búger than Carapelle, karst areas of the Búger headwater catchment caused a high threshold for runoff generation due to high transmission losses (Calvo-Cases et al., 2003). In addition, the spatial distribution of land uses in the Búger –forests at headwaters and agriculture in lowlands– reduced R, as the steepest part of the catchment (i.e., headwaters) is covered by natural vegetation, which increases rainfall interception (Buendia et al., 2016). In the Carapelle, 80% of the catchment is covered by seasonal crops, with arable land the driver for R generation (Cerdan et al., 2004). The medium size and elongated shape of the Carapelle, due to the heterogenization of

Table 5
Pearson correlation matrix for the Búger catchment. Significant correlation at $p < 0.05$ (italics) and $p < 0.01$ (bold)

	P_{tot}	$IP_{max}30$	AP1d	AP3d	Q_{dur}	Q_0	Q_{max}	FI	R	R_c	SSC_{max}	SFI	SSY
P_{tot}	1	0.30	0.36	**0.61**	0.20	−0.05	0.18	−0.25	0.37	0.02	0.32	−0.15	0.14
$IP_{max}30$		1	−0.18	−0.04	*−0.51*	−0.29	−0.14	**0.70**	−0.18	−0.35	0.02	**0.66**	−0.11
AP1d			1	**0.87**	*0.42*	**0.56**	**0.58**	−0.35	**0.76**	**0.64**	*0.49*	−0.29	**0.55**
AP3d				1	0.33	**0.54**	**0.58**	−0.33	**0.74**	**0.58**	**0.51**	−0.25	**0.54**
Q_{dur}					1	0.01	0.01	**−0.65**	0.29	0.20	−0.12	**−0.69**	0.00
Q_0						1	**0.82**	−0.22	**0.80**	**0.96**	**0.65**	−0.03	**0.78**
Q_{max}							1	−0.15	**0.91**	**0.81**	**0.84**	0.04	**0.99**
FI								1	−0.30	−0.33	−0.12	**0.87**	−0.11
R									1	**0.87**	**0.76**	−0.14	**0.88**
R_c										1	**0.62**	−0.16	**0.76**
SSC_{max}											1	0.15	**0.85**
SFI												1	0.08
SSY													1

Correlation $p < 0.01$.
Correlation $p < 0.05$.

Table 6
Pearson correlation matrix for the Carapelle catchment. Significant correlation at $p < 0.05$ (italics) and $p < 0.01$ (bold).

	P_{tot}	$IP_{max}30$	AP1d	AP3d	Q_{dur}	Q_0	Q_{max}	FI	R	R_c	SSC_{max}	SFI	SSY
P_{tot}	1	**0.77**	0.17	−0.11	**0.72**	0.10	**0.54**	−0.12	**0.62**	*−0.42*	0.29	0.03	*0.50*
$IP_{max}30$		1	0.36	0.10	0.28	0.24	**0.77**	0.22	**0.60**	−0.40	*0.52*	0.28	**0.60**
AP1d			1	*0.461**	−0.13	0.10	0.36	0.19	0.15	−0.08	0.31	0.13	0.19
AP3d				1	−0.04	0.28	0.27	−0.01	0.24	0.34	0.02	−0.05	0.24
Q_{dur}					1	0.23	0.30	**−0.61**	**0.66**	−0.21	−0.09	−0.40	*0.46*
Q_0						1	*0.46*	−0.38	**0.62**	0.09	0.18	−0.32	*0.43*
Q_{max}							1	0.10	**0.85**	−0.21	*0.49*	0.07	**0.88**
FI								1	−0.23	−0.21	*0.51*	**0.81**	0.01
R									1	−0.15	0.37	−0.16	**0.91**
R_c										1	−0.13	−0.28	−0.11
SSC_{max}											1	**0.63**	**0.54**
SFI												1	0.01
SSY													1

Correlation $p < 0.01$.
Correlation $p < 0.05$.

precipitations, influenced the streamflow. In such catchments, rainfall events of the same magnitude may generate different Q, depending on their distribution (García-Rama et al., 2016). These results confirm the research of López-Tarazón and Estrany (2017) and Pagano et al. (2019), who pointed out that comparing catchments with different features leads to better studies of the hydrological regime. However, among all the features of basins, geology, land cover, soil type and slope were relevant drivers of hydrological processes, partitioning waters between horizontal and vertical pathways (i.e. overland flow, infiltration) and determining the connectivity of the drainage network and storage (Chiverton et al., 2015; Borg Galea et al., 2019). Thus, due to the above-mentioned factors, the Búger River was characterized by greater flow intermittence and lower R_a.

The statistical relationships between the selected HIs and sediment transport regime indicators, along with the analysis of the hysteretic loops, indicate that hydrology was the most important sediment transport driver. On the annual scale, the SSY recorded in the Búger (0.5–46 t km^{-2} y^{-1}) indicated sediment delivery lower than the average rate of soil erosion (200–400 t km^{-2} y^{-1}) generally recorded in the Mediterranean region as reported by Van Rompaey et al. (2005), and also lower than the values for Spain (Avendaño Salas et al., 1997; De Vente et al., 2005; Vanmaercke et al., 2011). However, the annual SSY was similar to the soil formation rate (i.e., 0.2–55 t km^{-2} y^{-1}) observed in karst areas (Cao et al., 2020). In the Carapelle catchment, the SSY (89–745 t km^{-2} y^{-1}) was higher than the rate of soil formation of 140 t km^{-2} y^{-1} (Panagos et al., 2015; Verheijen et al., 2009). Ricci et al. (2019, 2018) highlighted that the soil erosion rate is critical in the basin, where catchment management is needed to reduce soil erosion. The large number of terraces in the Búger catchment contributes to decreasing water and sediment fluxes and preventing sediment detachment from the slopes, thus causing low amounts of SSY (Calsamiglia et al., 2018).

At the event scale, the close correlation between FI and SFI means that in Búger the increment or reduction of SY follows variations of Q, whereas in the Carapelle the low correlation observed between these variables indicates that sediment can be released later than the runoff peak. This result is confirmed by counter-clockwise and complex hysteresis loops characterizing the Italian basin.

Overall, 48 flood events were analysed for the Búger (25) and Carapelle (23) basins. In the Búger, the pre-event variables (i.e., AP1d, AP3d, and Q_0) meant that the drivers for runoff response confirmed previous studies (Estrany et al., 2010; Lana-Renault et al., 2007; Latron and Gallart, 2007). Furthermore, accordingly to Lana-Renault et al. (2007) and Fortesa et al. (2020a), seasonality was a key factor as all events with runoff > 4.9 mm occurred from December to February (the wet season). In addition, rainfall events between 36 and 46 mm had runoff yields between 0.04 and 4.9 mm. Among these events, a greater response in runoff and Q_{max} was seen in events with antecedent rainfall events, especially in the winter months. As in the Búger, the importance of favourable conditions over Q_{max} was reported in other Mediterranean catchments where antecedent wet soil conditions generated the greatest Q_{max} (Estrany et al., 2010; Zoccatelli et al., 2019). The importance of pre-event conditions suggests that runoff response is most probably the result of saturation excess processes (Dunne and Black, 1970). However, infiltration excess overland flow occurs in late spring and summer when precipitation exceeds the infiltration capacity of the soil (see events 6, 7, 8, 13, 25 in Fig. 4a).

Discriminant analysis indicated that in the Carapelle, R generation and Q_{max} were clearly influenced by P_{tot} (Latron et al., 2008) and $IP_{max}30$ (Manus et al., 2009), which were more significant than the pre-event variables. This behaviour is probably due to both rainfall characteristics (local and intense) and soil features (low permeability). However, the number of gauging stations in the basin is low, use of the Thiessen polygons to calculate the mean precipitation could lead to missing some important information (i.e. spatial distribution). Indeed, the hydrological response for rainfall events between 11 and 18.4 mm was non-linear, as observed in other Mediterranean basins (Latron et al., 2008; López-Tarazón et al., 2010). The highest values of R were recorded in events with very high Q_{max} (i.e., 100 m^3 s^{-1}) due to the combination of the total amount and the intensity of the rainfall event.

In the Búger, most of the SSY was transported during flood events characterized by high R and Q_{max}, which controlled large SSY and SSC_{max} values. These were the situations of greatest sediment transport, as they were very energetic events (López-Tarazón and Estrany, 2017). Analogous with the hydrological response, these events occurred under wet antecedent conditions (i.e., AP1d, AP3d and Q_0), as moisture conditions, not rainfall intensities, promoted the main runoff and sediment load contributions (Fortesa et al., 2020b; Seeger et al., 2004). However, 72% of the SSC_{max} was < 0.5 g l^{-1} and only in 5 events was a SSY > 1 t km^{-2} recorded. This was because of low sediment availability due to the karst coverage at the headwater's catchment (Li et al., 2019).

In the Carapelle, rainfall amount and intensity controlled the SSY contribution (high correlation coefficients) in the events with SSY > 200 t km^{-2}. In addition, the larger area of the Carapelle could be a factor explaining the high temporal and spatial rainfall variability (Ricci et al., 2018). This factor may explain the lack of correlation that was found in the Carapelle for the FI and SFI, due to a longer concentration time than in the Búger (Fig. 6). Furthermore, Q_{max} was a good indicator of the highest SSC_{max} and SSY, as pointed out by Duvert

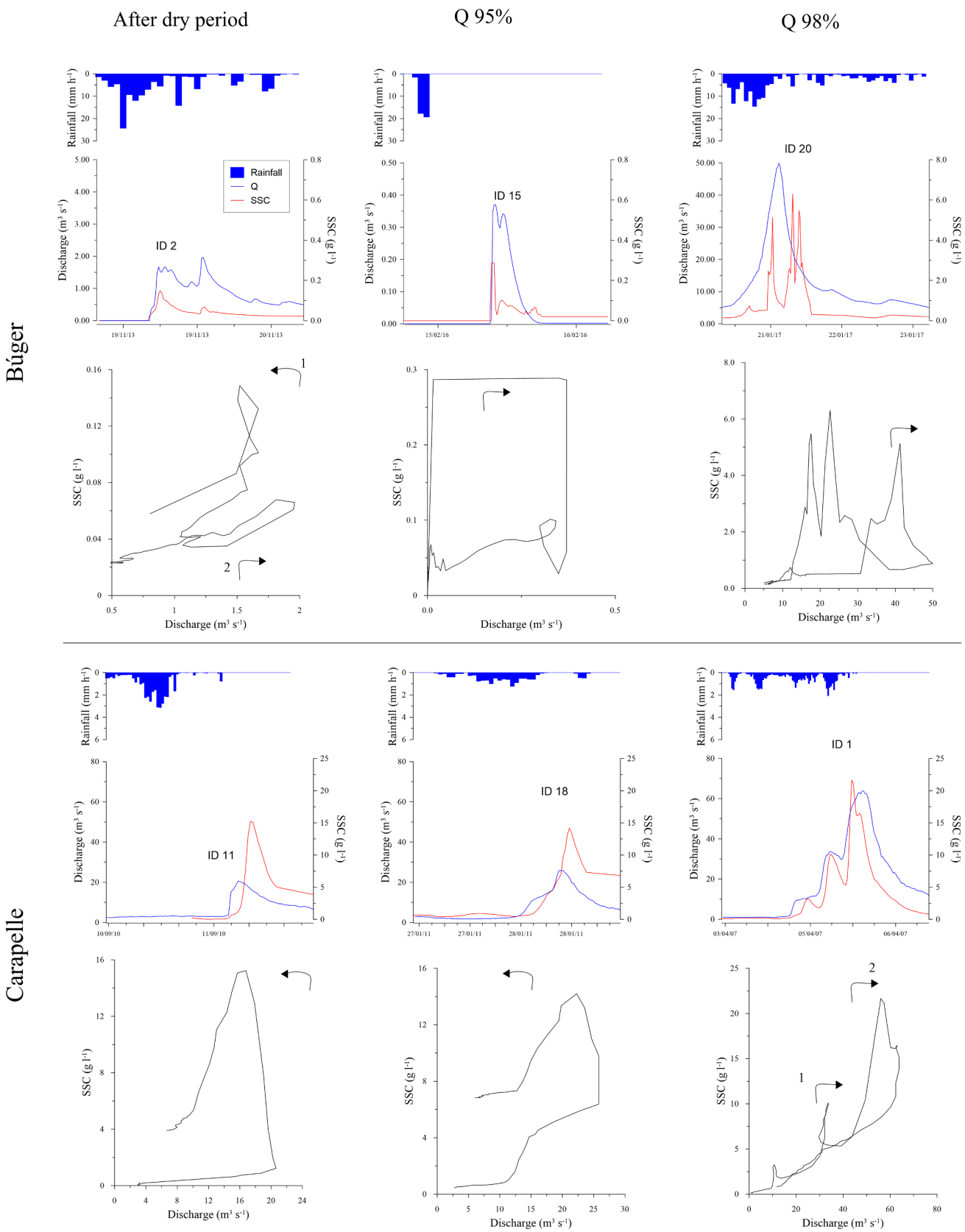

Fig. 6. Rainfall, discharge and suspended sediment concentration for the selected events on the Búger and Carapelle rivers and their respective hysteresis.

et al. (2012).

The Búger had predominantly clockwise loops, while in the Carapelle the counter-clockwise loops were more frequent. This difference occurs for several reasons, such as the size of the catchment, the pattern and distribution of the rainfall and the geological characteristics (Smith and Dragovich, 2009). Smaller catchments like the Búger are usually characterized by the prevalence of clockwise loops (Bezak et al., 2016; García-Rama et al., 2016) because the lag between Q and SSC decreases in small catchments and when the rainfall event is close to the gauging station (Heidel, 1956). The lithology of the headwaters, which is composed of 27.7% limestone (Table B1, Appendix B), allows the infiltration of rainfall and limits the detachment of sediment. Carbonate rocks and karst features promote low R and SSY due to high transmission losses and low SS availability (Li et al., 2019). Furthermore, the forested areas at the headwaters reduced soil detachment, protected by rainfall interception. In general, forest causes a decrease in annual values of 20% in R and 80% in SSY (Buendia et al., 2016). Lowland areas, characterised by agricultural land uses, were more exposed to the impact of rainfall drops causing larger amounts of R and SSY (Zuazo and Pleguezuelo, 2008). Hence, the sediment sources that most contribute to SY are the areas close to the outlet of the basin. This feature is often associated with clockwise behaviour (García-Rama et al., 2016). Moreover, the conservation practices adopted in the Búger (i.e. terraces and check-dams) played an important role in reducing sediment availability (Estrany et al., 2012). Therefore, it can be assessed that clockwise hysteresis is mostly related to the fine material detached from the streambed (De Girolamo et al., 2015b). Accordingly, the contributions of the water treatment plant may be favourable to clockwise hysteresis behaviour due to the direct spills into the streambed. The Carapelle, being a medium-size catchment, showed a predominance of counter-clockwise loops since the catchment has an elongated shape and some concentrated rainfall events occur far from the outlet, increasing the lag between Q and SSC (García-Rama et al., 2016). The extensive agricultural activity, where conventional practices included ploughing up and down the slopes, and the fine composition of the soils (Table B1, Appendix B) led to sediment generation from source areas all over the study site (De Girolamo et al., 2015b; García-Rama et al., 2016; Ricci et al., 2020). The greater presence of agricultural fields in the Carapelle than in the Búger promoted higher R and SSY due to the predominance of bare soils with low vegetation cover (Lana-Renault et al., 2014; Romano et al., 2018). Moreover, sediment was also supplied by processes of streambed erosion detected in some areas of the catchment that caused by the malfunction of the broken check-dams (Ricci et al., 2019). This high availability of sediment is frequently related to counter-clockwise behaviour (López-Tarazón and Estrany, 2017). For big storms, the Carapelle showed clockwise loops confirming that in semi-arid environments, like Mediterranean areas, intense rainfall caused clockwise hysteresis (Alexandrov et al., 2007; Brasington and Richards, 2000).

5. Conclusions

The relevance of the different degrees of flow intermittence to river ecosystems led to an evaluation of the flow regime's effects on sediment transport in two Mediterranean streams during a 5-year study period. By using HIs, the Búger and Carapelle streams were classified by flow occurrence and seasonal predictability: the two streams were Intermittent-Dry and Intermittent-Pool, respectively.

lithology and geological characteristics were found to be the main drivers controlling the hydrological regime and river type classification, while rainfall was less relevant. The hydrological regime was the most important driver of SS transport. The many terraces in the Búger catchment contributed to the sediments being retained. Meanwhile, agricultural management practices in the Carapelle made a lot of sediment liable to erosion. Indeed, the high SSY recorded in the Carapelle (89–745 t km^{-2} y^{-1}) indicated a critical soil erosion rate in the basin, while in the Búger the SSY was lower than the rate generally recorded in the Mediterranean region.

Most of SY was transported during extreme flood events. At the event scale, the SY recorded in the Carapelle was up to 4 orders of magnitude greater than in the Búger. Non-linearity in the rainfall-runoff relationship was found for both catchments. Runoff response may be due to saturation or infiltration excess. In the Búger, SSY and SSC_{max} correlated with the runoff, peak discharge and antecedent rainfall; whereas, in the Carapelle, SSY and SSC_{max} correlated with the amount and intensity of rainfall.

Hysteretic loops provide useful information concerning the source of sediment. Loops are greatly affected by the size, shape, lithology and land uses of the basins. A prevalence of clockwise loops for the Búger indicated that the sediment sources contributing to the SY are areas close to the outlet of the basin. Counter-clockwise loops prevailed in the Carapelle where the whole basin contributed to the SY.

Characterization of the flow regime of Mediterranean catchments and of its main physical drivers will help us to improve our understanding of the variability of the hydrological response and sediment transport of Intermittent Rivers and Ephemeral Streams (IRES).

Declaration of Competing Interest

The authors declare that they have no known competing financial interests or personal relationships that could have appeared to influence the work reported in this paper.

Acknowledgements

This work was supported by the Spanish Ministry of Science and Innovation, the Spanish Agency of Research (AEI) and the European Regional Development Funds (ERDF) through the project CGL2017-88200-R "Functional hydrological and sediment connectivity at Mediterranean catchments: global change scenarios –MEDhyCON2". The project "Soil Erosion in Apulia: Monitoring, Modelling and Control Strategies" was undertaken and performed within University of Bari and funded by the Apulia Basin Authority. J. Fortesa has a contract funded by the Vice-presidency and Ministry of Innovation, Research and Tourism of the Autonomous Government of the Balearic Islands [FPI/2048/2017; MOB_017]. G.F. Ricci received support from COST Action CA15113 (SMIRES, Science and Management of Intermittent Rivers and Ephemeral Streams). J. García-Comendador is in receipt of a contract [FPU15/05239] funded by the Spanish Ministry of Education and Culture. Meteorological data were facilitated by the Spanish Meteorological Agency (AEMET) and the Department of Civil Protection-National Hydrographic Service.

Appendix A

See Fig. A.1.

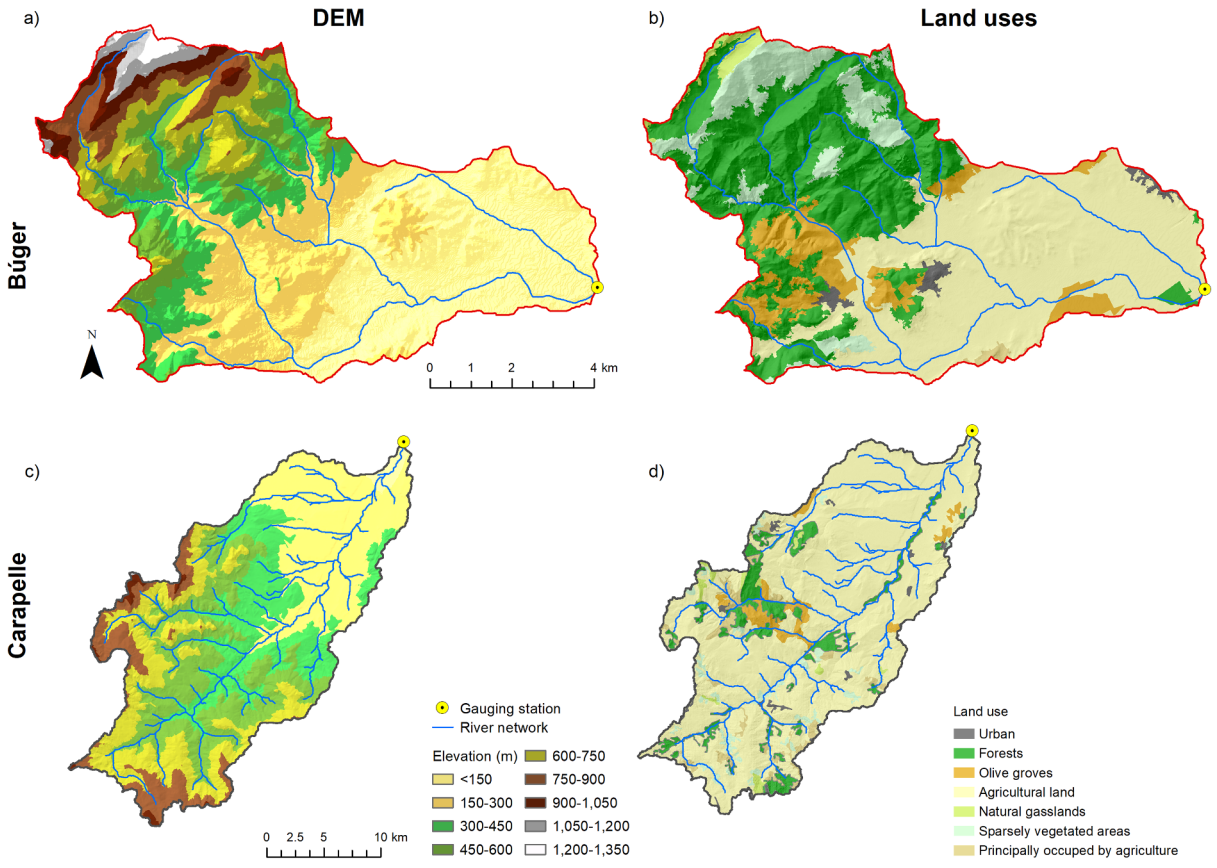

Fig. A1. Digital Elevation Models (a and c) and land uses cover (b and d) of both Búger and Carapelle catchment.

Appendix B

See Tables B1 and B2.

Table B1
Lithology of Búger and Carapelle catchments.

Búger lithology	(%)	Carapelle lithology	(%)
Silt, clays and gravels	29.7	Flyschoid units	39.0
Massive limestone and breccias	27.7	Sands and conglomerates	21.4
Conglomerates and limestone	16.1	Clays	16.1
Limestones and marls	14.5	Alluvial Terrace	11.0
Marls	9.8	Clays and marls sometimes with olistostromas	5.9
Bioclastic limestones and marls	1.7	Debris, Alluvial Terrace	3.0
Clays, evaporites and marls	0.4	Sandstone and Clays	2.5
		Sandstone-Marly units	1.1

Table B2
Land use % based on Corine Land Cover 2012.

Corine Land Cover 2012	Búger %	Carapelle %
Agricultural land	43.7	79.5
Forests	34.9	8.4
Sparsely vegetated areas	9.5	3.0
Olive groves	9.0	3.2
Natural grasslands	1.3	1.2
Urban	1.3	1.1
Land principally occupied by agriculture with significant areas of natural vegetation	0.4	3.6

References

Acuña, V., Datry, T., Marshall, J., Barceló, D., Dahm, C., Ginebreda, A., MCGregor, G., Sabater, S., Tockner, K., Palmer, M., 2014. Why should we care about temporary waterways? Science (80-.). 343, 1080–1081. https://doi.org/10.1093/biosci/bit027.

Alexandrov, Y., Laronne, J.B., Reid, I., 2007. Intra-event and inter-seasonal behaviour of suspended sediment in flash floods of the semi-arid northern Negev, Israel. Geomorphology 85, 85–97. https://doi.org/10.1016/j.geomorph.2006.03.013.

Arscott, D.B., Larned, S., Scarsbrook, M.R., Lambert, P., 2010. Aquatic invertebrate community structure along an intermittence gradient: Selwyn River, New Zealand. J. North Am. Benthol. Soc. 29, 530–545. https://doi.org/10.1899/08-124.1.

Avendaño Salas, C., Cobo Rayán, R., Sanz Montero, E., Gómez Montaña, J., 1997. Capacity situation in Spanish reservoirs. In: Dix-Neuvième Congrès Des Grands Barrages. Commission Internationale Des Grands Barrages, Florence.

Baker, D.B., Richards, R.P., Loftus, T.T., Kramer, J.W., 2004. A new flashiness index: characteristics and applications to Midwestern rivers and streams. J. Am. Water Resour. Assoc. 40, 503–522. https://doi.org/10.1111/j.1752-1688.2004.tb01046.x.

Berkun, M., Aras, E., 2012. River sediment transport and coastal erosion in the south-eastern Black Sea rivers / Transport riečnych sedimentov a erózia pobrežia riek krajiny v juhovýchodnej časti čierneho mora in: Journal of Hydrology and Hydromechanics Volume 60 Issue 4 (2012). Hydrol. Hydromech. 60, 299–308.

Bezak, N., Šraj, M., Mikoš, M., 2016. Analyses of suspended sediment loads in Slovenian rivers. Hydrol. Sci. J. 61, 1094–1108. https://doi.org/10.1080/02626667.2015.1006230.

Bisantino, T., Gentile, F., Milella, P., Trisorio Liuzzi, G., 2010. Effect of time scale on the performance of different sediment transport formulas in a semiarid region. J. Hydraul. Eng. 136, 56–61. https://doi.org/10.1061/(ASCE)HY.1943-7900.0000125.

Borg Galea, A., Sadler, J.P., Hannah, D.M., Datry, T., Dugdale, S.J., 2019. Mediterranean Intermittent Rivers and Ephemeral Streams: challenges in monitoring complexity. Ecohydrology. https://doi.org/10.1002/eco.2149.

Brasington, J., Richards, K., 2000. Turbidity and suspended sediment dynamics in small catchments in the Nepal Middle Hills. Hydrol. Process. 14, 2559–2574. https://doi.org/10.1002/1099-1085(20001015)14:14<2559::AID-HYP114>3.0.CO;2-E.

Buendia, C., Bussi, G., Tuset, J., Vericat, D., Sabater, S., Palau, A., Batalla, R.J., 2016. Effects of afforestation on runoff and sediment load in an upland Mediterranean catchment. Sci. Total Environ. 540, 144–157. https://doi.org/10.1016/j.scitotenv.2015.07.005.

Calsamiglia, A., Fortesa, J., García-Comendador, J., Lucas-Borja, M.E., Calvo-Cases, A., Estrany, J., 2018. Spatial patterns of sediment connectivity in terraced lands: Anthropogenic controls of catchment sensitivity. L. Degrad. Dev. 29, 1198–1210. https://doi.org/10.1002/ldr.2840.

Calvo-Cases, A., Boix-Fayos, C., Imeson, A., 2003. Runoff generation, sediment movement and soil water behaviour on calcareous (limestone) slopes of some Mediterranean environments in southeast Spain. Geomorphology 50, 269–291. https://doi.org/10.1016/S0169-555X(02)00218-0.

Cao, L., Wang, S., Peng, T., Cheng, Q., Zhang, L., Zhang, Z., Yue, F., Fryer, A.E., 2020. Monitoring of suspended sediment load and transport in an agroforestry watershed on a karst plateau, Southwest China. Agric. Ecosyst. Environ. 299, 106976. https://doi.org/10.1016/j.agee.2020.106976.

Cerdan, O., Le Bissonnais, Y., Govers, G., Lecomte, V., van Oost, K., Couturier, A., King, C., Dubreuil, N., 2004. Scale effect on runoff from experimental plots to catchments in agricultural areas in Normandy. J. Hydrol. 299, 4–14. https://doi.org/10.1016/j.jhydrol.2004.02.017.

Chiverton, A., Hannaford, J., Holman, I., Corstanje, R., Prudhomme, C., Bloomfield, J., Hess, T.M., 2015. Which catchment characteristics control the temporal dependence structure of daily river flows? Hydrol. Process. 29, 1353–1369. https://doi.org/10.1002/hyp.10252.

Costigan, K.H., Kennard, M.J., Leigh, C., Sauquet, E., Boulton, A.J., 2017. Flow regimes in intermittent rivers and ephemeral streams. Intermittent Rivers Ephemer. Streams 51–78. https://doi.org/10.1016/B978-0-12-803835-2.00003-6.

Custodio, E., Llamas, M., 2005. Idrologia Sotterranea. Palermo.

D'Ambrosio, E., De Girolamo, A.M., Barca, E., Ielpo, P., Rulli, M.C., 2017. Characterising the hydrological regime of an ungauged temporary river system: a case study. Environ. Sci. Pollut. Res. 24, 13950–13966. https://doi.org/10.1007/s11356-016-7169-0.

Datry, T., Bonada, N., Boulton, A., 2017. General introduction. In: Intermittent Rivers and Ephemeral Streams: Ecology and Management. Academic Press, pp. 1–597. https://doi.org/10.1016/B978-0-12-803835-2.00001-2.

Datry, T., Larned, S.T., Tockner, K., 2014. Intermittent rivers: A challenge for freshwater ecology. Bioscience. https://doi.org/10.1093/biosci/bit027.

De Girolamo, A., Lo Porto, A., Pappagallo, G., Tzoraki, O., Gallart, F., 2015a. The hydrological status concept: application at a temporary river (Candelaro, Italy). River Res. Appl. 31, 892–903. https://doi.org/10.1002/rra.2786.

De Girolamo, A., Pappagallo, G., Lo Porto, A., 2015b. Temporal variability of suspended sediment transport and rating curves in a Mediterranean river basin: The Celone (SE Italy). CATENA 128, 135–143. https://doi.org/10.1016/j.catena.2014.09.020.

De Girolamo, A.M., Di Pillo, R., Lo Porto, A., Todisco, M.T., Barca, E., 2018. Identifying a reliable method for estimating suspended sediment load in a temporary river system. Catena 165, 442–453. https://doi.org/10.1016/j.catena.2018.02.015.

De Vente, J., Poesen, J., Verstraeten, G., 2005. The application of semi-quantitative methods and reservoir sedimentation rates for the prediction of basin sediment yield in Spain. J. Hydrol. 305, 63–86. https://doi.org/10.1016/j.jhydrol.2004.08.030.

Dunne, T., Black, R.D., 1970. Partial area contributions to storm runoff in a small New England watershed. Water Resour. Res. 6, 1296–1311. https://doi.org/10.1029/WR006i005p01296.

Duvert, C., Nord, G., Gratiot, N., Navratil, O., Nadal-Romero, E., Mathys, N., Némery, J., Regüés, D., García-Ruiz, J.M., Gallart, F., Esteves, M., 2012. Towards prediction of suspended sediment yield from peak discharge in small erodible mountainous catchments (0.45–22 km2) of France, Mexico and Spain. J. Hydrol. 454–455, 42–55. https://doi.org/10.1016/J.JHYDROL.2012.05.048.

EC, 2000. EU Water Framework Directive.

Estrany, J., Garcia, C., Batalla, R.J., 2010. Hydrological response of a small mediterranean agricultural catchment. J. Hydrol. 380, 180–190. https://doi.org/10.1016/j.jhydrol.2009.10.035.

Estrany, J., Garcia, C., Martínez-Carreras, N., Walling, D.E., 2012. A suspended sediment budget for the agricultural Can Revull catchment (Mallorca, Spain). Zeitschrift für Geomorphol. Suppl. Issues 56, 169–193. https://doi.org/10.1127/0372-8854/2012/S-00110.

Estrany, J., Garcia, C., Walling, D.E., Ferrer, L., 2011. Fluxes and storage of fine-grained sediment and associated contaminants in the Na Borges River (Mallorca, Spain). Catena 87, 291–305. https://doi.org/10.1016/j.catena.2011.06.009.

Fortesa, J., García-Comendador, J., Calsamiglia, A., López-Tarazón, J.A., Latron, J., Alorda, B., Estrany, J., 2019. Comparison of stage/discharge rating curves derived from different recording systems: Consequences for streamflow data and water management in a Mediterranean island. Sci. Total Environ. 665, 968–981. https://doi.org/10.1016/J.SCITOTENV.2019.02.158.

Fortesa, J., Latron, J., García-Comendador, J., Tomàs-Burguera, M., Company, J., Calsamiglia, A., Estrany, J., 2020a. Multiple temporal scales assessment in the hydrological response of small Mediterranean-climate catchments. Water 12. https://doi.org/10.3390/w12010299.

Fortesa, J., Latron, J., García-Comendador, J., Company, J., Estrany, J., 2020b. Runoff and soil moisture as driving factors in suspended sediment transport of a small mid-mountain Mediterranean catchment. Geomorphology 368. https://doi.org/10.1016/j.geomorph.2020.107349.

Gallart, F., Prat, N., Garca-Roger, E.M., Latron, J., Rieradevall, M., Llorens, P., Barbera, G.G., Brito, D., De Girolamo, A.M., Lo Porto, A., Buffagni, A., Erba, S., Neves, R., Nikolaidis, N.P., Perrin, J.L., Querner, E.P., Quinonero, J.M., Tournoud, M.G., Tzoraki, O., Skoulikidis, N., Gamez, R., Gomez, R., Froebrich, J., 2012. A novel approach to analysing the regimes of temporary streams in relation to their controls on the composition and structure of aquatic biota. Hydrol. Earth Syst. Sci. 16, 3165–3182. https://doi.org/10.5194/hess-16-3165-2012.

Gamvroudis, C., Nikolaidis, N.P., Tzoraki, O., Papadoulakis, V., Karalemas, N., 2015. Water and sediment transport modeling of a large temporary river basin in Greece. Sci. Total Environ. 508, 354–365. https://doi.org/10.1016/j.scitotenv.2014.12.005.

García-Comendador, J., Fortesa, J., Calsamiglia, A., Calvo-Cases, A., Estrany, J., 2017. Post-fire hydrological response and suspended sediment transport of a terraced Mediterranean catchment. Earth Surf. Process. Landforms 42. https://doi.org/10.1002/esp.4181.

García-Rama, A., Pagano, S.G., Gentile, F., Lenzi, M.A., 2016. Suspended sediment transport analysis in two Italian instrumented catchments. J. Mt. Sci. 13, 957–970. https://doi.org/10.1007/s11629-016-3858-x.

Gentile, F., Bisantino, T., Corbino, R., Milillo, F., Romano, G., Liuzzi, G.T., 2010. Monitoring and analysis of suspended sediment transport dynamics in the Carapelle torrent (Southern Italy). Catena 80, 1–8. https://doi.org/10.1016/j.catena.2009.08.004.

GOIB, 2020. Portal de l'aigua de les Illes Balears [WWW Document]. Depuració d'aigües residuals. URL https://www.caib.es/sites/aigua/ca/depuracio_daigues_residuals-42698/.

Heidel, S.G., 1956. The progressive lag of sediment concentration with flood waves. Trans. Am. Geophys. Union 37, 56. https://doi.org/10.1029/TR037i001p00056.

INE, 2019. Instituto Nacional de Estadística. (Spanish Statistical Office) [WWW Document]. Demogr. Popul. Munic. Regist. Popul. by Munic. URL https://www.ine.es/dyngs/INEbase/en/categoria.htm?c=Estadistica_P&cid=1254734710990 (accessed 2.12.20).

Jaeger, K.L., Sutfin, N.A., Tooth, S., Michaelides, K., Singer, M., 2017. Geomorphology and Sediment Regimes of Intermittent Rivers and Ephemeral Streams. Intermittent Rivers Ephemer. Streams 21–49. https://doi.org/10.1016/B978-0-12-803835-2.00002-4.

Kannan, N., Anandhi, A., Jeong, J., 2018. Estimation of stream health using flow-based indices. Hydrology 5, 20. https://doi.org/10.3390/hydrology5010020.

Kottek, M., Grieser, J., Beck, C., Rudolf, B., Rubel, F., 2006. World Map of the Köppen-Geiger climate classification updated. Meteorol. Zeitschrift 15, 259–263. https://doi.org/10.1127/0941-2948/2006/0130.

Lana-Renault, N., Latron, J., Regüés, D., 2007. Streamflow response and water-table dynamics in a sub-Mediterranean research catchment (Central Pyrenees). J. Hydrol. 347, 497–507. https://doi.org/10.1016/J.JHYDROL.2007.09.037.

Lana-Renault, N., Nadal-Romero, E., Serrano-Muela, M.P., Alvera, B., Sánchez-Navarrete, P., Sanjuan, Y., García-Ruiz, J.M., 2014. Comparative analysis of the response of various land covers to an exceptional rainfall event in the central Spanish Pyrenees, October 2012. Earth Surf. Process. Landforms 39, 581–592. https://doi.org/10.1002/esp.3465.

Larned, S.T., Datry, T., Arscott, D.B., Tockner, K., 2010. Emerging concepts in temporary-river ecology. Freshw. Biol. https://doi.org/10.1111/j.1365-2427.2009.02322.x.

Latron, J., Gallart, F., 2007. Seasonal dynamics of runoff-contributing areas in a small mediterranean research catchment (Vallcebre, Eastern Pyrenees). J. Hydrol. 335, 194–206. https://doi.org/10.1016/J.JHYDROL.2006.11.012.

Latron, J., Soler, M., Llorens, P., Gallart, F., 2008. Spatial and temporal variability of the hydrological response in a small Mediterranean research catchment (Vallcebre, Eastern Pyrenees). Hydrol. Process. 22, 775–787. https://doi.org/10.1002/hyp.6648.

Li, Z., Xu, X., Zhu, J., Xu, C., Wang, K., 2019. Effects of lithology and geomorphology on sediment yield in karst mountainous catchments. Geomorphology 343, 119–128.

https://doi.org/10.1016/j.geomorph.2019.07.001.
López-Tarazón, J., Batalla, R.J., Vericat, D., Balasch, J.C., 2010. Rainfall, runoff and sediment transport relations in a mesoscale mountainous catchment: The River Isábena (Ebro basin). CATENA 82, 23–34. https://doi.org/10.1016/J.CATENA.2010.04.005.
López-Tarazón, J.A., Estrany, J., 2017. Exploring suspended sediment delivery dynamics of two Mediterranean nested catchments. Hydrol. Process. 31, 698–715. https://doi.org/10.1002/hyp.11069.
Manus, C., Anquetin, S., Braud, I., Vandervaere, J.-P., Creutin, J.-D., Viallet, P., Gaume, E., 2009. Hydrology and Earth System Sciences A modeling approach to assess the hydrological response of small mediterranean catchments to the variability of soil characteristics in a context of extreme events, Hydrol. Earth Syst. Sci.
Oueslati, O., De Girolamo, A.M., Abouabdillah, A., Kjeldsen, T.R., Lo Porto, A., 2015. Classifying the flow regimes of Mediterranean streams using multivariate analysis. Hydrol. Process. 29, 4666–4682. https://doi.org/10.1002/hyp.10530.
Pagano, S.G., Rainato, R., García-Rama, A., Gentile, F., Lenzi, M.A., 2019. Analysis of suspended sediment dynamics at event scale: comparison between a Mediterranean and an Alpine basin. Hydrol. Sci. J. 64, 948–961. https://doi.org/10.1080/02626667.2019.1606428.
Panagos, P., Borrelli, P., Poesen, J., Ballabio, C., Lugato, E., Meusburger, K., Montanarella, L., Alewell, C., 2015. The new assessment of soil loss by water erosion in Europe. Environ. Sci. Policy 54, 438–447. https://doi.org/10.1016/j.envsci.2015.08.012.
Poff, N.L., Allan, J.D., Bain, M.B., Karr, J.R., Prestegaard, K.L., Richter, B.D., Sparks, R.E., Stromberg, J.C., 1997. The natural flow regime. Bioscience 47, 769–784. https://doi.org/10.2307/1313099.
Prat, N., Gallart, F., Von Schiller, D., Polesello, S., García-Roger, E.M., Latron, J., Rieradevall, M., Llorens, P., Barberá, G.G., Brito, D., De Girolamo, A.M., Dieter, D., Lo Porto, A., Buffagni, A., Erba, S., Nikolaidis, N.P., Querner, E.P., Tournoud, M.G., Tzoraki, O., Skoulikidis, N., Gómez, R., Sánchez-Montoya, M.M., Tockner, K., Froebrich, J., 2014. The mirage toolbox: an integrated assessment tool for temporary streams. River Res. Appl. 30, 1318–1334. https://doi.org/10.1002/rra.2757.
Ricci, G.F., De Girolamo, A.M., Abdelwahab, O.M.M., Gentile, F., 2018. Identifying sediment source areas in a Mediterranean watershed using the SWAT model. L. Degrad. Dev. 29, 1233–1248. https://doi.org/10.1002/ldr.2889.
Ricci, G.F., Jeong, J., De Girolamo, A.M., Gentile, F., 2020. Effectiveness and feasibility of different management practices to reduce soil erosion in an agricultural watershed. Land Use Policy 90, 104306. https://doi.org/10.1016/j.landusepol.2019.104306.
Ricci, G.F., Romano, G., Leronni, V., Gentile, F., 2019. Effect of check dams on riparian vegetation cover: A multiscale approach based on field measurements and satellite images for Leaf Area Index assessment. Sci. Total Environ. 657, 827–838. https://doi.org/10.1016/j.scitotenv.2018.12.081.
Richter, B.D., Baumgartner, J.V., Powell, J., Braun, D.P., 1996. A method for assessing hydrologic alteration within ecosystems. Conserv. Biol. 10, 1163–1174. https://doi.org/10.1046/j.1523-1739.1996.10041163.x.
Romano, G., Abdelwahab, O.M.M., Gentile, F., 2018. Modeling land use changes and their impact on sediment load in a Mediterranean watershed. Catena 163, 342–353. https://doi.org/10.1016/j.catena.2017.12.039.
Sauquet, E., Richard, B., Devers, A., Prudhomme, C., 2019. Water restrictions under climate change: a Rhône-Mediterranean perspective combining bottom-up and top-down approaches. Hydrol. Earth Syst. Sci. 23, 3683–3710. https://doi.org/10.5194/hess-23-3683-2019.
Sauquet, E., van Meerveld, I., Gallart, F., Sefton, C., Parry, S., Gauster, T., Laaha, G., Alves, M.H., Arnaud, P., Banasik, K., Beaufort, A., Bezdan, A., Datry, T., De Girolamo, A.M., Dörflinger, G., Elçi, A., Engeland, K., Estrany, J., Fialho, A., Fortesa, J., Hakoun, V., Karagiozova, T., Kohnova, S., Kriauciuniene, J., Morais, M., Ninov, P., Osuch, M., Reis, E., Rutkowska, A., Stubbington, R., Tzoraki, O., Żelazny, M., 2020. A catalogue of European intermittent rivers and ephemeral streams. https://doi.org/10.5281/ZENODO.3763419.
Schick, P.A., 1967. Suspended sampler and bedload trap. F. methods study slope Fluv. Process. Rev. Geormorphologie Dyn. 17, 181–182.
Sear, D.A., Armitage, P.D., Dawson, F.H., 1999. Groundwater dominated rivers. Hydrol. Process. 13, 255–276. https://doi.org/10.1002/(SICI)1099-1085(19990228)13:3<255::AID-HYP737>3.0.CO;2-Y.
Seeger, M., Errea, M.-P., Beguería, S., Arnáez, J., Martí, C., García-Ruiz, J.., 2004. Catchment soil moisture and rainfall characteristics as determinant factors for discharge/suspended sediment hysteretic loops in a small headwater catchment in the Spanish pyrenees. J. Hydrol. 288, 299–311. https://doi.org/10.1016/J.JHYDROL.2003.10.012.
Sherriff, S.C., Rowan, J.S., Fenton, O., Jordan, P., Melland, A.R., Mellander, P.E., Huallacháin, D., 2016. Storm event suspended sediment-discharge hysteresis and controls in agricultural watersheds: implications for watershed scale sediment management. Environ. Sci. Technol. 50, 1769–1778. https://doi.org/10.1021/acs.est.5b04573.
Skoulikidis, N.T., Sabater, S., Datry, T., Morais, M.M., Buffagni, A., Dörflinger, G., Zogaris, S., del Mar Sánchez-Montoya, M., Bonada, N., Kalogianni, E., Rosado, J., Vardakas, L., De Girolamo, A.M., Tockner, K., 2017. Non-perennial Mediterranean rivers in Europe: Status, pressures, and challenges for research and management. Sci. Total Environ. https://doi.org/10.1016/j.scitotenv.2016.10.147.
Smakhtin, V.U., 2001. Low flow hydrology: A review. J. Hydrol. https://doi.org/10.1016/S0022-1694(00)00340-1.
Smith, H.G., Dragovich, D., 2009. Interpreting sediment delivery processes using suspended sediment-discharge hysteresis patterns from nested upland catchments, south-eastern Australia. Hydrol. Process. 23, 2415–2426. https://doi.org/10.1002/hyp.7357.
Van Rompaey, A., Bazzoffi, P., Jones, R.J.A., Montanarella, L., 2005. Modeling sediment yields in Italian catchments. Geomorphology 65, 157–169. https://doi.org/10.1016/j.geomorph.2004.08.006.
Vanmaercke, M., Poesen, J., Verstraeten, G., de Vente, J., Ocakoglu, F., 2011. Sediment yield in Europe: Spatial patterns and scale dependency. Geomorphology 130, 142–161. https://doi.org/10.1016/j.geomorph.2011.03.010.
Vercruysse, K., Grabowski, R.C., Rickson, R.J., 2017. Suspended sediment transport dynamics in rivers: Multi-scale drivers of temporal variation. Earth-Science Rev. https://doi.org/10.1016/j.earscirev.2016.12.016.
Verheijen, F.G.A., Jones, R.J.A., Rickson, R.J., Smith, C.J., 2009. Tolerable versus actual soil erosion rates in Europe. Earth-Science Rev. https://doi.org/10.1016/j.earscirev.2009.02.003.
Vericat, D., Batalla, R.J., 2006. Sediment transport in a large impounded river: The lower Ebro, NE Iberian Peninsula. Geomorphology 79, 72–92. https://doi.org/10.1016/j.geomorph.2005.09.017.
Williams, G., 1989. Sediment concentration versus water discharge during single hydrologic events in rivers. J. Hydrol. 111, 89–106.
Wohl, E., Bledsoe, B.P., Jacobson, R.B., Poff, N.L., Rathburn, S.L., Walters, D.M., Wilcox, A.C., 2015. The natural sediment regime in rivers: Broadening the foundation for ecosystem management. Bioscience. https://doi.org/10.1093/biosci/biv002.
YACU, 2002. Estudio de caracterización del régimen extremo de precipitaciones en la isla de Mallorca. Junta d'Aigües de les Illes Balears, Palma de Mallorca.
Zoccatelli, D., Marra, F., Armon, M., Rinat, Y., Smith, J.A., Morin, E., 2019. Contrasting rainfall-runoff characteristics of floods in desert and Mediterranean basins. Hydrol. Earth Syst. Sci 23, 2665–2678. https://doi.org/10.5194/hess-23-2665-2019.
Zuazo, D.V., Pleguezuelo, C., 2008. Soil-erosion and runoff prevention by plant covers. A review. Agron. Sustain. Dev 28, 65–86. https://doi.org/10.1051/agro:2007062.

Glossary

AP1d: Antecedent precipitation 1 day before (mm)
AP3d: Antecedent precipitation 3 day before (mm)
BFI: Base Flow Index
DH1: Maximum annual flow of 1-day duration
DL6: Number of zero days
E: Episodic-ephemeral
FDC: Flow Duration Curve
Fdi: Multi-annual frequencies of zero-flow months for the contiguous six wetter months
Fdj: Multi-annual frequencies of zero-flow months for the remaining six drier months
FI: Richards-Baker Flashiness Index
I-D: Intermittent-dry
IHA: Indicators of Hydrologic Alteration
I-P: Intermittent-pools
$IP_{max}30$: Maximum 30′ precipitation intensity (mm h^{-1})
IRESs: Intermittent Rivers and Ephemeral Streams
P: Perennial
P_{tot}: Total precipitation (mm)
Q_{dur}: Flood duration (h)
Q_{max}: Peak discharge (m^3 s^{-1})
R: Runoff (mm)
R_a: Annual Runoff (mm y^{-1})
R_c: Runoff coefficient (%)
SD6: 6-month seasonal predictability of dry periods
SDC: Sediment Duration Curve
SFI: Sediment Flashiness Index
SSC: Suspended Sediment Concentration (g l^{-1})
SSC_{max}: Maximum suspended sediment concentration (g l^{-1})
SSY: Specific Sediment Yield (t km^{-2} y^{-1})
SY: Sediment yield (t)
TH1: Date of maximum flow
TL1: Date of minimum flow